UNITED NATIONS EDUCATIONAL, SCIENTIFIC AND CULTURAL ORGANIZATION
INTERNATIONAL ATOMIC ENERGY AGENCY
INTERNATIONAL CENTRE FOR THEORETICAL PHYSICS
I.C.T.P., P.O. BOX 586, 34100 TRIESTE, ITALY, CABLE: CENTRATOM TRIESTE

H4.SMR/1058-10

WINTER COLLEGE ON OPTICS

9 - 27 February 1998

Interaction of Light and Matter in the Optical Near Field

V. Sandoghdar

Fakultät für Physik, Universität Konstanz, Germany

Interaction of Light and Matter in the Optical Near Field

Winter College on Optics
International Center for Theoretical Physics
Trieste, Italy

9 -26 February 1998

Vahid Sandoghdar

Fakultät für Physik
Universität Konstanz
Konstanz, Germany

email: vahid.sandoghdar@uni-konstanz.de

Course Outline

I. Introduction/Motivation

II. An atom/molecule in front of a mirror

a) A classical radiating dipole in front of a perfect mirror
b) A classical radiating dipole in front of an imperfect mirror
c) A free quantum mechanical atom
d) A quantum mechanical atom in front of a mirror

III. Optical detection and spectroscopy of single molecules

a) Single molecule detection with a SNOM
b) Single molecule detection in far field

IV. Nanoscopic light bulbs as novel probes for SNOM

a) Single molecules
b) Small volumes of fluorescing material
c) Luminescence from semiconductors

V. Scanning optical near-field lithography (SNOL)

a) Conventional photoresist
b) Radical polymerization
c) Tungsten oxide
d) Overview of SNOL
e) Microfabrication as a possible solution for the future of SNOL

VI. Closing Remarks

I. Introduction

The fascination with the world of constituents of matter is an old topic dating to many thousand years ago. The advent of optical elements such as lenses allowed the realization of the first family of microscopes, namely the optical microscope, which we still use today. The early microscope allowed a deeper look into our surroundings and facilitated several important discoveries in science such as discovery of biological micro-organism and of the brownian motion. By the late nineteenth century the theoretical foundation of classical electromagnetism was well understood and the limits of the optical microscopy formulated. The wave nature of light at wavelength λ dictates a limit of the order of $\lambda/2$ on the ultimate localization or focusing of light known as the "diffraction limit". With the birth of quantum mechanics and the concept of matter waves it was a natural step to employ material particles as probes for examining matter. Such massive particles have large momenta and therefore a small de Broglie wavelength leading to a higher achievable resolution in microscopy. Today various techniques based on electron beams such as Scanning Electron Microscopy (SEM) or Transmission Electron Microscopy (TEM) are commercially available which allow a resolution of one nanometer or better.

For about a decade there has been an explosion of interest in other methods of high resolution microscopy. This trend is certainly motivated to a great extend by the growing interest in miniaturization and microfabrication of semiconductor devices as well as information storage. The central role of high resolution microscopy methods in these activities is two fold. First one utilizes microscopy for diagnostics and testing of the fabrication processes. More fundamentally, the limits and methodology of nanofabrication are determined by the physics behind the various microscopy methods. For example, diffraction of light which puts a limit on the resolution in microscopy is exactly the phenomenon responsible for the limits in conventional optical lithography. Therefore, new methods of microscopy also mean new avenues for local modification of matter, namely lithography.

The economic motors behind nanofabrication have also resulted in a need to understand the underlying physics of such mesoscopic systems. Phenomena such as electric transport or optical luminescence of structures much smaller than 100nm are heavily influenced by the quantum effects resulting from the finite structure size. For example the confinement of electron wavefunctions to a region of 5nm leads to a large change of the emission spectrum in semiconductor luminescence [Waggon]. At such a small scale it is worth noting that the structure consists of only a few hundred atoms in each direction, and one requires new methods for understanding and describing the optical or electrical properties. From the fabrication point of view the meeting of the classical bulk and single particle quantum worlds can be realized either by an up-down approach typically used in lithography or by a bottom-up approach of making molecules from single atoms and quantum dots from single molecules, etc. Such horizons are also currently motivating some of the current research in physics and chemistry.

As the size and local morphology of the structure play an important role in the physics, an access to this information is desirable in the experiment. One can do this by using ensembles of particles in two steps. One first examines the geometry by

performing for example electron microscopy and then studies the optical or electrical properties of the sample, trying to correlate the two. However, often a more direct approach is needed in order to understand the details of the problem. Experiments on single systems instead of ensembles are therefore very interesting, especially if one can collect all this information simultaneously. In atomic physics several groups have aimed at studying single ions or atoms by manipulating them in an electromagnetic trap [Monroe, et al.]. Biophysicist and physical chemists have succeeded in detecting single molecules [Moerner], and in semiconductor physics one is now able to perform experiments on single quantum dots [Gammon, et al.].

The focus of this school is on optics, I have decided to tell you about the interaction of light and matter in the optical near field. I will assume a basic knowledge of the principles and instrumentation of Scanning Near-field Optical Microscopy (SNOM) since Professor Van Labeke has already introduced this topic to you. SNOM is a particularly interesting and promising tool because it allows optical spectroscopy with a high spatial resolution. It is important to emphasize that the strength of SNOM is not just to "look" at small things but more to probe the internal structure of matter by spectroscopy on a nanometer scale. It turns out though that near-field spectroscopy implies being very close to surfaces. So I will start by discussing what happens when an atom or a molecule gets very close to a surface. We will see that the lifetime and the energy levels of the atom are influenced. This will set the grounds for what we will see when we discuss the state of the art microscopy and spectroscopy on single molecules using near-field optics. After this I would like to convince you that there are still other novel methods of optical near-field microscopy on the verge of development with the hope of pushing the obtainable resolution to its limits. As a last main topic, I will show some examples of lithography in the optical near field emphasizing the current problems and future directions.

In writing these note I have kept a very brief style considering them more as supplements and reminders to the lectures. The list of references are also not very exhaustive. When possible I have referenced review articles or books where the interested reader can follow up on the details or find new sources of information. On top of these, there are some topics which I have left out in order to have more time for the basics. One of these is the area of near-field spectroscopy on semiconductors, especially single quantum dots, wires, etc [see for example Gammon et al.]. This line of research has been one of the main driving forces of SNOM but will only become seriousely interesting when the resolution surpasses 20-50nm. Another topic that I will not touch upon is proposals and some experiments on apertureless SNOM based on local scattering of the near field by tiny scatter centers at the tip [see for example Zennhausern et al.94]. Finally, there has been also some recent experiments on Second Harmonic Generation (SHG) in the near field [see the work of Davis]. These ideas are very fascinating and promising but beyond the scope of a short course. Inspite of the shortcomings mentioned, I hope you will get a flavor of some of the ideas and directions which are currently being developed in the area of optical near-field microscopy and spectroscopy.

II. An atom/molecule in front of a mirror

It is now well established that the radiative properties of an atom are modified when they are in the vicinity of surfaces. The possibility of changing the lifetime of the excited state in an atom, or in other words the linewidth of its transition was first pointed out by Purcell [Purcell] in 1946. He argued that by changing the density of states of the modes of vacuum into which the atom can emit a photon, one can modify the rate at which the atom emits. As we will see, exactly this happens when an atom is placed close to a mirror. The fact that atoms experience a force and therefore a change of energy levels was known much before that to those studying adsorption and van der Waals effects in gases [Margenau].

We will spend some time here reviewing the important aspects of these issues emphasizing the state of the art experimental verification of these effects. Although at the first sight there might not be any connection between optical near field microscopy or spectroscopy and such issues usually treated in quantum electrodynamics, you will see that they recur many times while discussing experiments such as the detection of single molecules with SNOM. In a nut shell it is helpful to discuss this topic because one is always forced to work very close to surfaces when performing experiments in the optical near field. Moreover, it turns out that a quantum mechanical atom behaves quite similar to a radiating dipole moment in many circumstances. Therefore, we will start our discussion by first considering the problem of a dipole moment in front of a mirror. We will then point out some subtle differences between a classical dipole and an atom.

Consider the radiation produced by the dipole $\mathbf{p}e^{-i\omega t}$ (see fig.1). The electric field $\mathbf{E}(\mathbf{r})$ produced at position $\mathbf{r}$ is given by [Jackson],

$$\vec{E}(\vec{r}) = \frac{k^3 e^{ikr} e^{-i\omega t}}{4\pi\varepsilon_0} \left\{ (\hat{n}\times\vec{p})\times\hat{n}\left(\frac{1}{kr}\right) + \left[3\hat{n}(\hat{n}\cdot\vec{p}) - \vec{p}\right]\left(\frac{1}{(kr)^3} - \frac{i}{(kr)^2}\right)\right\}$$

where $\vec{r} = \hat{n} r$

(1)

when $r>>\lambda$ one obtains the familiar far field radiation

$$\vec{E}_{far} \longrightarrow k^2(\hat{n}\times\vec{p})\times\hat{n}\ \frac{e^{ikr}}{r}\ e^{-i\omega t},$$

and in the near field (when $r<<\lambda$) one arrives at the non-propagating field

$$\vec{E}_{near} \longrightarrow \left[3\hat{n}(\hat{n}\cdot\vec{p}) - \vec{p}\right]\frac{1}{r^3}\ e^{-i\omega t}$$

The time-averaged radiated power $\mathcal{P}_0$ can be obtained by integrating the Poynting vector and is given by,

$$\mathcal{P}_0 = \frac{c k^4}{12\pi\varepsilon_0} |\vec{p}|^2 \tag{2}$$

where k is the wavevector.

II.a A classical radiating dipole in front of a perfect mirror

Imagine having placed the dipole **p** a distance z away from a perfect conductor (see fig.2). The radiation emitted by the dipole is now reflected from the mirror and acts back on itself. The reflected electric field can be calculated from equation (1) by replacing kr with the round trip phase $2kz=\phi$ and taking into account a π phase shift for $\mathbf{E}_{\mathrm{I}}^{\mathrm{refl.}}$,

$$\vec{E}_{\parallel}^{\,refl} = \frac{\vec{p}_{\parallel} k^3 e^{i\phi}}{4\pi\varepsilon_0}\left[-\frac{1}{\phi} - \frac{i}{\phi^2} + \frac{1}{\phi^3}\right] e^{-i\omega t}$$

$$\vec{E}_{\perp}^{\,refl} = \frac{\vec{p}_{\perp} k^3 e^{i\phi}}{2\pi\varepsilon_0}\left[-\frac{i}{\phi^2} + \frac{1}{\phi^3}\right] e^{-i\omega t} \tag{3}$$

The power dissipated due to the interaction of the reflected field and the dipole is the time derivative of the imaginary part of the hamiltonian giving [Hinds, Morawitz]

$$\Delta\mathcal{P} = \mathrm{Im}\left(\vec{p}\cdot\vec{E}^{*refl}\right)\frac{\omega}{2}$$

$$\Rightarrow \quad \Delta\mathcal{P}_{\perp} = \frac{3}{2}\mathcal{P}_0\left[-\frac{\sin\phi}{\phi} - \frac{\cos\phi}{\phi^2} + \frac{\sin\phi}{\phi^3}\right]$$

$$\Delta\mathcal{P}_{\parallel} = 3\mathcal{P}_0\left[-\frac{\cos\phi}{\phi^2} + \frac{\sin\phi}{\phi^3}\right] \tag{4}$$

The change of energy (directly related to its oscillation frequency) of the dipole is obtained from the real part of the interaction hamiltonian [Haroche]

$$\Delta\mathcal{E} = -\frac{1}{2}\mathrm{Re}\left(\vec{p}\cdot\vec{E}^{*refl}\right)$$

$$\Delta\mathcal{E}_{\perp} = \frac{k^3}{4\pi\varepsilon_0}\left[|\vec{p}_{\perp}|^2\left(-\frac{\sin\phi}{\phi^2} - \frac{\cos\phi}{\phi^3}\right)\right]$$

$$\Delta\mathcal{E}_{\parallel} = \frac{k^3}{8\pi\varepsilon_0}\left[|\vec{p}_{\parallel}|^2\left(\frac{\cos\phi}{\phi} - \frac{\sin\phi}{\phi^2} - \frac{\cos\phi}{\phi^3}\right)\right] \tag{5}$$

Figures 3 and 4 plot the normalized change in the radiated power as well as the change in the dipole's energy as a function of its separation z from the mirror. Note that we could have just as well considered the interaction of the oscillating dipole with the electric field produced by its mirror image (see fig. 5)

$$\vec{p}'_{\parallel} = -\vec{p}_{\parallel} \quad ; \quad \vec{p}'_{\perp} = \vec{p}_{\perp}$$

The signs introduced here are equivalent to the phase shifts we considered upon reflection of the incident field on the mirror. It is then easy to see that the oscillation in these plots are simply the results of the periodic variations of the phase between **p** and the field of its image. Now let us look at the asymptotic behavior of this energy shift

$z \ll \lambda/\pi$

$$\Delta\mathcal{E}_{near} \longrightarrow \frac{-k^3}{8\pi\varepsilon_0}\left[\frac{2|p_\perp|^2 + |p_\parallel|^2}{\phi^3}\right] = \frac{-1}{64\pi\varepsilon_0}\left[\frac{2|p_\perp|^2 + |p_\parallel|^2}{z^3}\right] \quad (6)$$

$z \gg \lambda/\pi$

$$\Delta\mathcal{E}_{far} \longrightarrow \frac{-k^3}{8\pi\varepsilon_0}\left[2\frac{|p_\perp|^2 \sin\phi}{\phi^2} + \frac{|p_\parallel|^2 \cos\phi}{\phi}\right] \quad (7)$$

The first case (without the time average) is often referred to as the near field part and can be obtained simply from the electrostatic interaction energy of a dipole **p** with its image **p'** [Jackson]

$$W_{12} = \frac{\vec{p}\cdot\vec{p}' - 3(\hat{n}\cdot\vec{p})(\hat{n}\cdot\vec{p}')}{4\pi\varepsilon_0 (2z)^3} \quad \text{with } \hat{n} = \hat{z}.$$

II.b A classical radiating dipole in front of an imperfect mirror

Real metallic or dielectric mirrors are far from a perfect conductor. One usually has to take into account the absorption and dispersion of the reflector. This can be simply treated by considering a complex index of refraction for the substrate. For the calculations it means accounting for the finite reflectivity and phase shift of the field upon reflection. In other words, multiply equation (3) by a factor $\xi e^{i\delta}$. For a real metallic mirror with a small loss ($\delta \ll 1$) one obtains a behavior as shown in fig. 6. Note that at distances very close to the mirror the power dissipated diverges for both dipole orientations. The reason for this is the coupling of the near field with the electrons in the metal and dissipation of heat. Furthermore, at these distances the near field can couple to surface plasmons. A full treatment of the interaction of an emitter very close to a real surface goes beyond a simple electromagnetic interaction, and one has to look at the overlap between the electronic wavefunction in the metal, scattering of electrons from the surface, etc. Although in practice these issues have to be dealt with, we will not emphasize this point here and refer the interested reader to the review article by Ford and Weber [Ford &Weber] for a detailed discussion.

II.c A free quantum mechanical atom

Let us first consider an atom in free space. You might have noticed in your basic course on quantum mechanics that when one regards a hydrogen atom one can solve for the wavefunctions and eigenenergies, but they come out to be very stable. Yet we know from experience that an excited state usually decays within a fraction of milliseconds. This decay is often put into the solution afterwards phenomenologically. In order to arrive at this decay from first priciples, one has to takes into account the coupling of the atomic states to all the "empty" electromagnetic modes of the vacuum. In other words, one has to consider the effect of fluctuating vacuum fields associated with the zero-point energy of the quantized field [Loudon, Milonni]. One obtains then

$$\Gamma_a = \frac{|\vec{d}|^2 \omega_a^3}{3\pi\varepsilon_0 \hbar c^3} \qquad \text{where} \quad \vec{d} = \langle e|e\vec{r}|g\rangle \tag{8}$$

for the decay rate of the excited state. Since the unit of energy per decay is $\hbar\omega_a$, the "power" emitted is given by $\mathcal{P}_a = \hbar\omega_a \Gamma_a$

$$\mathcal{P}_a = \frac{ck^4}{3\pi\varepsilon_0} |\vec{d}|^2 \tag{9}$$

The broadening mentioned above is also accompanied by a small shift which was discovered in hydrogen for the first time by Lamb in 1947 [Lamb]. This shift is often interpreted as the AC Stark effect produced on the atomic state by the fluctuating fields in vacuum. Although we have emphasized the role of quantum fluctuations in describing the radiative porperties of a free atom, comparing the outcome of equation (9) with that of equation (2) one sees a huge similarity (up to a factor of 4, or in other words, a factor of 2 between **d** and **p**). This correspondence between an atom and a classical radiating dipole is the reason why one often thinks of an atom simply as a dipole antenna. The small quantitative discrepancy mentioned above [Hinds&Sandoghdar] is very interesting and even important. However, as you will see shortly, in the optical near field we can consider an *excited* atom to be equivalent to a classical dipole moment. A rigorous treatment of these issues and their interpretations are reviewed recently by P. Milonni [Milonni].

II.d A quantum mechanical atom in front of a mirror

Now let us come to the case of an atom in front of a mirror. One can write down the complete quantum mechanical hamiltonian of the atom and the field taking care of the boundary conditions that have to be satisfied at the interface [Haroche, Hinds]. The full expression is cumbersome so that below we only consider its asymptotic behavior for a 2-level atom.

Excited State

a) $z \gg \lambda/\pi$ (far field)

$$\delta_e^{far} \longrightarrow \frac{ka^3}{4\pi\varepsilon_0}\left[\frac{2|\vec{d}_\perp|^2 \sin\phi}{\phi^2} - \frac{|\vec{d}_{||}|^2 \cos\phi}{\phi}\right] \qquad (10)$$

b) $z \ll \lambda/\pi$ (near field)

$$\delta_e^{near} \longrightarrow \frac{1}{64\pi\varepsilon_0}\left[\frac{2|\vec{d}_\perp|^2 + |\vec{d}_{||}|^2}{z^3}\right]$$

Ground State

a) $z \gg \lambda/\pi$ (far field)

$$\delta_g^{far} \longrightarrow \frac{1}{64\pi\varepsilon_0}\,\frac{|\vec{d}|^2}{ka \cdot z^4} \qquad (11)$$

b) $z \ll \lambda/\pi$ (near field)

$$\delta_g^{near} \longrightarrow \frac{1}{64\pi\varepsilon_0}\left[\frac{2|\vec{d}_\perp|^2 + |\vec{d}_{||}|^2}{z^3}\right]$$

Note that the average dipole moment in a given atomic state is zero and yet one ends up with a dipole-dipole interaction. The answer to this puzzling situation is again the quantum mechanical fluctuations of the observable **r** or in other words **d**=*e***r**. Although

$$\langle g|\vec{d}|g\rangle = 0,$$

one has $\langle g|\vec{d}^2|g\rangle \neq 0$.

One can explain this intuitively by thinking of the system having a dipole moment which interacts at any given instant with its image in the mirror, i.e. if the propoagation time $t \ll 2z/c$ is very short [Lennard-Jones]. This is also the explanation behind the van der Waals interaction between two atoms or molecules. The story of this interaction goes back to the discovery of capillary forces [see Margenau] in the early eighteenth century. Many great scientists such as Laplace, Gauss, Maxwell, Boltzmann, van der Waals and Debye tried to understand the nature of forces between neutral bodies, but without any real success. The first breakthrough came after the invention of quantum mechanics. In 1930 F. London used perturbation theory to treat the electrostatic interaction between two neutral atoms. In this manner he explained the van der Waals energy and forces, but it turned out that the correct solution had to take into account the retardation in propagation of photongs. This was shown first in 1948 by Casimir and Polder [Casimir&Polder]. In the near region they found exactly the solution given by London/Lennard-Jones theory but far from the mirror they discovered a difference distance dependence (see remark (4) below).

Remark (1) In the near zone the ground state and the excited state shift by the same amount and proportional to $1/z^3$. This is not exactly the case for real many level atoms although the $1/z^3$ dependence will still persist.

Remark (2) The excited state behaves qualitatively and almost quantitatively like a classical dipole moment. This is because there is a real dipole moment $\mathbf{d}=\langle g|\mathbf{r}|e\rangle$ associated with the atom.

Remark (3) Even the excited state and classical dipole don't agree quantitatively for all z [Hinds&Sandoghdar].

Remark (4) The ground state behaves very differently for large distances $z \gg \lambda/\pi$. The distance dependence is faster and like $1/z^4$. This is due to a retardation effect or in other words, the finite speed of light. The fluctuations of the dipole moment are no longer in phase with the reflected field. Furthermore, since the quantum fluctuations of the dipole moment do not have a well-defined frequency (as is the case for the excited state or for a classical dipole moment) the interaction of the dipole with its reflected field doesn't oscillate. In their 1948 paper Casimir and Polder quantized the electromagnetic field as well as the atom and showed that the $1/z^3$ dependence of the London/Lennard-Jones interaction breaks down when $z \gg \lambda/\pi$. Incidentally together with the experimental discopvery of Lamb this was the first evidence that the zero point energy in quantum mechanics can have a physical meaning.

From the experimental point of view there have been many indirect evidence of such interactions over the years. However, it was only recently that a direct spectroscopic measurement of the Lennard-Jones/van der Waals energy was made [Sandoghdar et al. 92, & 96]. The reason is that the shifts are very small (about a few 10 kHz for sodium ground state at a distance of several 100nm) and also because of the need for precise positioning of the atom in front of the mirror. Figure 7 shows experimental data (symbols) obtained by a direct comparison of the energy levels of sodium atoms between two gold mirrors with those of sodium in free space. The schematics of the setup was as shown in fig. 8. Atoms were excited to low-lying Rydberg states in order to magnify the interaction energy which is proportional to the square of the dipole moment. The solid curves are calculated from equations 10 and 11 in the limit of near field without any free parameters. This was the first time that the different aspects of the Lennard-Jones van der Waals interaction were tested systematically and precisely in one experiment. Again, it is important to emphasize this point to appreciate the difficulties which are involved in performing controlled experiments very close to surfaces.

The first conclusive measurement of the force between the atom and a mirror in the "far" distance regime was done by the same group and setup as in fig. 8 [Sukenik et al.]. A spectroscopic measurement of this effect was no longer possible and instead the force was put into evidence. Atoms were sent into the parallel-plate cavity and the number of those which survived the mirror forces was counted. Figure 9 shows the inverse of the atom counts as a function of mirror separation. A clear deviation from a purely static Lennar-Jones force was demonstrated.

The above-mentioned experiments all aimed at studying the energies or forces. Now let us look at the decay rates for atoms. A quantum mechanical calculation gives

$$\Gamma_{\parallel} = \Gamma_a + \frac{3}{2}\left\{-\frac{\sin\Phi}{\Phi} - \frac{\cos\Phi}{\Phi^2} + \frac{\sin\Phi}{\Phi^3}\right\}$$

$$\Gamma_{\perp} = \Gamma_a + 3\left\{-\frac{\cos\Phi}{\Phi^2} + \frac{\sin\Phi}{\Phi^3}\right\} \qquad (12)$$

These are identical to the results in eq. (4) if one replaces $\mathcal{P}_0$ with Γ_a.

Remark (5) For a real atom the ground state is stable and doesn't decay. Therefore, the results in eq. (11) are for the excited state. So once again we find that the excited state of a quantum mechanical atom is just like a classical radiating dipole.

Up to now we have looked at the modification of the radiative properties of an atom/molecule near a surface. You saw that depending on whether one is close or far from the mirror the picture of the atom-mirror interaction changes. We are particularly interested in the "near" regime here where the interaction can be regarded as electrostatic. Furthermore, it was shown above that in this region that the analogy between an atom and an oscillating dipole is essentially exact. In the next sections we will see that these plays a central role in optical near-field microscopy both in the interpretation of the observed phenomena and in devising novel methods of optical microscopy.

III. Optical detection and spectroscopy of single molecules

One of the most exciting achievements of SNOM has been the high resolution detection and spectroscopy of single molecules. Many of us were told in high school that a molecule is too small to be seen even by the best microscopes. The difficulty of detecting or "seeing" a single molecule is of course first its very small size (typically 1-10Å), but this can be these days overcome by methods such as Atomic Force Microscopy (AFM) [Jung et al.] or Scanning Tunneling Microscopy [Stroscio&Eigler]. The direct optical measurement of a single molecule is for that very reason still not possible though.

A second problem is the signal-to-noise ratio S/N. In other words, the amount of light coming from a single molecule is usually so small that it is lost in the noise. It was shown in 1993 that one can overcome this problem by performing the experiment in the optical near field [Betzig&Chichester]. Since then it has been also demonstrated that one can actually do this in the far field by compromising the resolution. So let us take a closer look at some of these experiments.

III.a Single molecule detection with SNOM

The setup used is basically that of a SNOM plus a series of filters and photon counting detectors (see fig. 10). The sample is prepared by spin coating a dilute solution of a dye (concentration 10^{-8}-10^{-9}) onto a microscope objective. After letting the solution evaporate one is left with randomly distributed molecules with typical lateral separations of ~0,5-1μm. One then excites these molecules at λ_{exc} while scanning the SNOM probe very close to the sample. When the tip meets a dye molecule one detects its fluorescence at λ_{fluo} in transmission. By plotting the signal on the detector as a function of the scan position, one obtains images like in fig. 11.

A usual first question after having seen such an image is what is the proof that one really has a single molecule under the tip. Although for any given single molecule it is a difficult task to prove this, several arguments can be put forward in defense of this claim [Betzig&Chichester].

1) The # of molecules observed per μm^2 agrees with that expected from the initial concentration to within an order of magnitude.
2) The density of the observed light points changes linearly over 3 orders of magnitude with concentration.
3) The peak signal observed is consistent with that of a single dye molecule.
4) Bleaching doesn't occur gradually, but rather suddenly.
5) Each structure has a well-defined dipole orientation.

The S/N ratio in such experiments is typically 5-10. There are several limiting factors and problems:

1) One cannot excite the molecule at intensities close to saturation because input powers more than a few mW damage the metal coating of the tip. So one performs these experiments with a far field output of ~1-10nW from the tip.
2) This means that one needs to integrate 10-30 msec per pixel in order to get a good S/N. The result is a very slow scan and experiment. Typical scan time for a 1μmx1μm scan is about 10 minutes.
3) All dye molecules have limited lifetimes at room temperature due to various photophysical and photochemical bleaching processes. So one cannot very easily make repeated measurements on the same system.
4) In order to separate the fluorescence light from that of the excitation it is necessary to insert filters in the detection which always introduce some losses.
5) The collection solid angle as well as the quantum efficiencies of the detectors amount to only about 10-20%.
6) One has to often fight against stray fluorescence. In fact, in doing such experiments one discovers that almost everything in the lab fluoresces when excited in the green or blue. Most filters and immersion oils used in conventional microscopy fluoresce. In the case of a SNOM, however, one has two more sources of trouble. First the Raman lines of silica and second the fluorescence of the jacket on the optical fiber. The first has to be eliminated by proper filtering while the second one can be simply removed. It is generally a good idea to keep the fiber as short as possible (20-50cm).

Betzig also managed to extract enough information from such images to identify the orientation of the absorption dipole moment of the molecule. The intensity $I(x, y, \theta, \phi)$ detected from a point dipole at (x_0, y_0, z_0) on the sample and oriented along θ and ϕ (see fig.12) is given by

$$I(x,y,\theta,\varphi) = \Lambda(\theta,\varphi,\psi=\psi_0)\left|\vec{P}(x_0,\theta,\varphi)\cdot\vec{E}(x,y,z_0)\right|^2 \quad (13)$$

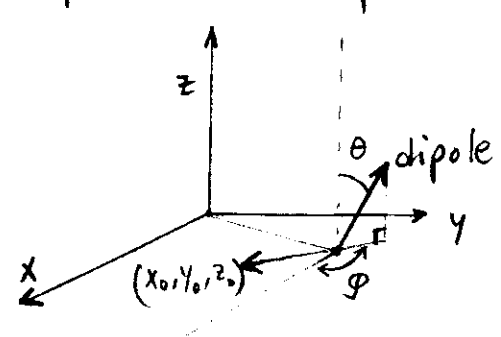

where ψ_0 is the collection angle (N.A.=$n.sin\psi$). Λ is a geometrical factor taking into account the radiation pattern of the dipole in the vicinity of an interface. We consider Λ to be constant, an assumption which is justified if ψ_0 is very large [Axelrod79].

Let us now assume that the excitation is linearly polarized in the tip. This is not very difficult to achieve from a typical SNOM tip out of a monomode fiber, but the extinction ratio one obtains depends on the details of the tip preparation. This was about 5:1 in the first experiment of Betzig, but values as high as 80:1 have been reported [Xie&Dunn94]. Usually, however, there is a direction of maximum extinction ratio making an on-commnad rotation of polarization impossible. In what follows we'll assume a linearly polarized excitation in the tip.

The polarization in the near field is quite complex. This is due to the fact that there are large longitudinal components in the non-propagating part leading to a highly non-uniform and spatially dependent fields (see fig. 13). Figure 14 shows the intensity distribution at several distances from an aperture of 100nm as calculated from the Bethe [Bethe] and Bouwkamp [Boukamp] (B&B) theory as well as two experimentally determined distributions in the middle [Betzig&Chichester]. Two molecules with point-like dipole moments along the far-field excitation polarization (top) and perpendicular to it (bottom) have been used to map out these intensity distributions[1].

In general the absorption dipole moment and the emission dipole moments are not parallel. In all the experiments reported so far, however, they have been within 20° of each other. At any rate, given a certain linear polarization in the tip one obtains the maximum fluorescence signal when the excitation is parallel to the absorption dipole moment. The orientation of the in-plane absorption dipole moment of a given molecule is then simply calculated via $I=I_{max}.cos^2\phi$. Note that a molecule with a large z-component of absorption dipole is characterized by its two-lobed fluorescence intensity pattern (see fig. 14). Furthermore, at the center of the tip $E_z=0$, and the signal is only due to the in-plane dipole moment. Once the in-plane absorption dipole is identified, Betzig used the results of the B&B theory shown in fig. 13 and 14 to extract the z-component by comparing the full intensity distribution pattern with those of the theory. Figure 15 shows the result of such an analysis. Note, however, thtat the accuracy of such an assignment is limited by the S/N ratio and cannot be very high in a near-field experiment.

One can also identify the orientation of the emission dipole. In order to do this one needs to simply examine the polarization state of the fluorescence of a single molecule. By rotating a polarization analyzer and comparing the intensity in each case one can deduce the emission dipole moment [Ruiter et al.97]. These experiments have been very exciting because one could essentially visualize a single molecule. Information such as real-time rotation or translation of single molecules can therefore be obtained [Ha et al.96a]. Such studies are very interesting because they give access

[1] The validity of the B&B theory was also recently put into evidence [Decca97] by scanning a 9nm wide strip of semiconductor to map out the field distribution at the tip.

to knowledge that one cannot get from ensembles. As mentioned before, however, the accuracy and the speed with which one can perform these experiments are determined by the S/N ratio and the integration time in detection. This is one of the biggest weak points of SNOM and the main reason why in the past 2-3 years many groups have traded the higher resolution of SNOM with the speed and ease of operation of confocal detection.

III.b Single molecule detection in far field

There will be lectures on confocal fluorescence microscopy later at this school, and I will not describe the details here. It suffices to say that one usually places the sample at the focus of a diffraction limited beam and detects the fluorescence back through the same microscope objective. In addition, by passing the detection through a pinhole one can also discriminate against stray light. This technique offers a diffraction limited resolution of the order of $\lambda/2$ which is only a factor of 3 or 4 worse than typical SNOM resolutions obtained. The first such experiment on single molecules sitting on a surface was reported in 1996 [Trautman&Macklin, Macklin et al.96]. Figure 16 shows the schematics of the hybrid near-field/far-field setup, and figure 17 shows some images taken in the far-field. Although we are mainly interested in near-field optics here, it is useful to compare the two techniques. The biggest advantages and disadvantages of SNOM in comparison to confocal microscopy are as follow:

SNOM Advantages	**SNOM Disadvantages**
• higher resolution	• non-reproducible tips
• smaller excitation volume; therefore lower background from the sample	• small intensities
• large longitudinal E-field to couple to $\mathbf{p}_z$	• slow scan
•	• Raman fluorescence of glass
•	• fiber jacket fluorescence
•	• difficult polarization control
•	• tip perturbation on the molecule:
	1. due to a high temperature
	2. change of molecules lifetime

The last point listed as a disadvantage actually attracted a lot of attention between 1994 and 1996 when several groups reported a tip-sample distance dependent modification of molecule's lifetimes. Given the earlier discussion we had in section II, it is not surprising that the proximity of the tip can introduce variations in the lifetime. Figure 18 shows the measured lifetimes for several molecules as a function of lateral displacement of the tip with respect to the molecule [Ambrose et al.94]. Qualitatively one can argue that the quenching of lifetime in front of the metal coating is due to the coupling to electrons in the metal as discussed before. From a theoretical point of view the analytical results obtained previously for the case of a molecule in front of an infinite mirror do not apply to this case where the diameter of the "mirror" is only $\sim\lambda/2$. Some numerical work has been done though addressing this issue [Gir., Novot]. As expected, one obtains a tip-sample distance dependent modification of the lifetime.

A quantitative study of the experimental observations based on first principle calculations are not really possible since the details of the tip geometry are not known. Also it is known that aluminum is always covered with a layer of oxide, making the system less ideal. The non-reproducibility of this lifetime change is emphasized in a paper by Trautman in 1996 [Trautman&Macklin]. He clearly states that depending on the details of tip preparation they can even nearly eliminate this effect. At any rate, although one can in principle think of the tip as a potential control parameter for the radiative properties of the molecule, this variation of the lifetime is more bothersome than helpful for studies in biology where one wants to identify a certain type of molecule by its lifetime.

Aside from the effects of the SNOM tip on the lifetime, it is also very important to study the variations in the lifetime of single molecules sitting on a surface or in a thin film, as commonly done in biology where one uses dye molecules as labels. Single molecules are very promising for high resolution labeling and therefore it is important to study their properties in comparison to those known from ensemble experiments.

Far field spectroscopy and detection is best suited for this purpose. The AT&T group has performed simultaneous measurements of the lifetimes as well as emission spectra of single molecules with their combined SNOM/confocal setup. They have reported several different situations. In some cases as shown in figure 19, the spectrum as well as the lifetime is essentially identical in the near and far field experiments (in contrast to the results of [Ambrose et al.94]). In some other cases the spectra of two molecules are shifted with respect to each other while having the same lifetime. They claim that most of the time, however, red-shifted molecules have longer lifetimes. They attributed this correlation (see fig. 20) to the inherent dependence of the spontaneous emission rate to the third power of transition frequency (see equation 8). The quality of the collected data is not so that this could be examined unambiguously.

Before closing this section it is worth mentioning a phenomenon now known as "blinking" [Betzig&Chichester, Dickson et al.97, Ruiter et al.97]. As shown in fig. 21, it happens that during a scan a molecule stops and resumes emitting after a certain time. The exact origin of this is not clear and most probably depends on the system. Some candidates could be spectral jumps, re-orientation of the absorption dipole moment, or trapping in metastable states. This characteristic which could happen on very short (sub-msec) or long (several minutes) time scales is yet another difficulty in using single molecules at room temperature for further experiments.

IV. Nanoscopic light bulbs as novel probes for SNOM

In previous sections we have discussed near-field detection or spectroscopy of single molecules on a surface. Here we will examine the possibility of using a single molecule or a tiny source of light to replace the aperture in the usual SNOM tips (see fig. 22). Since the resolution obtained in near field optics is limited by the size of the source, it is plausible to obtain an extremely high resolution by coupling a single molecule to a sample. The important point to remember here is that the resolution obtained is given by the strength of the available components of the k-vector and is therefore a sensitive function of the probe-sample distance. In other words, in order to

take advantage of the small size of a molecule, one needs to be essentially in contact with the sample.

IV.a Single molecules

In recent years there have been a few proposals suggesting the use of single molecules as ideal sources for optical near-field microscopy [Kopelman&Tan, Lewis95, Sekatskii&Letokhov]. Some of these ideas are based on resonant energy transfer from the probe molecule to the sample molecules. Here the short length scale of 4-8nm for energy transfer compared to ~100nm for photons is very helpful in getting a high resolution [Lieberman et al.90].

A particularly elegant contrast mechanism can be the modification of lifetime. As shown in fig. 23, imaging with high resolution should be possible by monitoring the lifetime of the probe molecule as positioned against the sample [Rahmani et al.97]. Another mechanism which we are studying at the moment is the energy level shifts of a single probe molecule as it is scanned on a sample.

The success in the realization of these ideas depend on several factors. First one has to position a single molecule at the foremost extremity of a tip in order to be able to scan real surfaces. Second, to perform controlled experiments, the molecule should live at least a few hours before bleaching. This rules out typical single molecule systems at ambient conditions. A possible avenue might be the use of methods developed in 1989 and 1990 [Moerner&Kador89, Orrit&Bernard90] for spectroscopy of single molecules in a solid (glassy or crystalline) matrix. The idea in this kind of experiment is to identify or detect a single molecule in frequency space. This becomes possible at T~1.7K where the homogeneous broadenings of individual molecules reduce to their natural linewidths. As a result, neighboring lines do not overlap and the spectrum consists of many well-resolved lines of 10-40 MHz. This corresponds to a quality factor of $\sim 10^7$ offering a very high sensitivity to small perturbations from the environment. Furthermore, bleaching is minimized at low temperatures. As shown in figure 24, one can then address single in a small crystal in frequency space and position it against the sample while observing the position and width of the resonance line. In this manner one will realize a stable and very sensitive point-like quantum system which can be manipulated with nanometric precision.

IV.b Small volumes of fluorescing material

On the way to the ultimate limit of molecular resolution in optical microscopy there has been some activity in the realization of apertureless SNOM based on the fluorescence of a very small volume at the extremity of a tip. The idea here is to examine the sample in the near field of the fluorescence from a nanoscopic light source just the same way that one exploits the near field of an aperture. The size of the source will determine the best possible resolution. There are several advantages of this system over the traditional metal-coated fiber tips. The excitation can in principle be done via far-field optics since it is the confinement of the fluorescence that is important and not that of the excitation. A second advantage is that there is no fundamental lower limit to the size of the active center in such a probe. This is in contrast to the case of metal-coated probes which become limited at the level of aluminum skin depth. Finally, the

intensity obtained from such probes scales more softly with the size than in the case of an aperture. For an aperture of diameter ϕ it is believed that $I \sim \phi^6$ while for such a probe $I \sim \phi^3$. Given that the fluorescence from a single molecule can be now detected, efficient detection of the signal from such probes with several thousand emitters should not pose any problems.

Already in 1990 A. Lewis and R. Kopelman produced sub-micron centers of a fluorescing crystal [Lieberman et al. 90] or dye-doped polymer [Lewis&Lieberman91] in the front of a metal coated sharp pipette (see fig. 25). Aside from the problems of bleaching, this method has several disadvantages which have prevented its development for resolutions under 100nm. First, the size of the probe is still determined by the preparation (pulling and coating) of the hollow pipette. This also means that the non-reproducibility of the tips persists. Finally, the metal coating is not desirable due to its quenching effects on the emitters.

More recently a group at Max-Planck-Institute for biophysical chemistry has reported on incorporating a dye-doped polymer layer at the tip of a polymer AFM tip [Jovin]. In Konstanz we have also developed a method for producing very small centers of polymer doped with Eu^{3+}. Figure 26 shows an electron microscope image of such a tip with a small center of $\phi \sim 200$nm. We are currently improving this to collect much smaller centers $\phi < 50$nm. The interesting aspect of this method is its promise for reducing the size in a controlled manner.

IV.c Luminescence from semiconductors

Similar ideas can be extended to luminescence from nanometric semiconductor probes. Here the exciting perspective is near field microscopy via electroluminescence; i.e. without the need of any laser. There have been a few reports on such efforts [Heckl95, Kuck et al.92, Granstroem et al.95] but so far no real success. The biggest problem, in addition to a systematic fabrication of such small active probes, is the proper contacting for electroluminescence. With the rapid progress of micro- and nano-fabrication it should be only a matter of time for these ideas to be executed.

V. Scanning optical near-field lithography (SNOL)

So far we have talked about examining the radiative properties of matter in the optical near field and also about novel methods where radiative properties of matter are exploited to learn about a sample; i.e. to perform microscopy. As is common, however, microscopy and lithography are very closely related, or in a certain sense are the opposite of each other. One can use an electron beam, ion beam, light beam or various scanning probe techniques to examine a sample or to modify it. Optical lithography is a particularly important technique because the microelectronics industry with a volume over 120 billion $ in 1996 relies fully on it for creating structures in 200-300nm range. This is typically done by covering the semiconductor with a polymer (photoresist) which reacts to light, similar to what happens to a camera film. One can then "write" a certain pattern into this thin film and use various etch methods to project the pattern to the underlying substrate. Since far field optics is diffraction limited, the only way to improve the resolution of this technique is to reduce the wavelength at which one modifies a surface. This avenue becomes somewhat dead-end

though once the wavelength goes well into the ultraviolet. The problem is not only generation of this light but also finding proper materials for lenses, mirrors and masks. So it would be very interesting to produce structures below the diffraction limit using visible or near UV light. This is possible using a SNOM tip to illuminate a sample. One has to remember, however, that since the optical near field has a very "shallow depth" one cannot expect to obtain very deep structures while maintaining their widths under 100nm.

V.a Conventional photoresist

We have performed such experiments in Konstanz resulting in structure widths as low as ~80nm [Wegscheider95]. In the first experiment we have illuminated a thin layer of conventional photoresist about 20nm thick using a metal-coated fiber tip. The light source was an argon-ion laser operating at λ=454nm. The sample was scanned under the tip and later developed. The illuminated area was then examined under an AFM. The profiles in the topography could be fit fairly well by a Gaussian and showed a FWHM as low as ~80nm (see fig. 27). The good Gaussian fit means that the sample was not well into to the near field as was the case for single molecules of Betzig. But this is not surprising since the sample has a finite thickness. Figure 28 shows the calculated field intensity at several distances from the tip. At a distance of 10nm the profile is already beginning to be close to a Gaussian. Note that 20nm away from the aperture the FWHM is ~80nm although the aperture diameter was taken to be 100nm. Similar experiments have also been reported by other groups [Davy96, for a review see Nyffenegger97].

V.b Radical polymerization

We have mentioned that a direct patterning process in the near field cannot lead to narrow and deep structures. One can in principle get around this by adding a second step in which one grows a film on top of the near-field-structured sample or where one etches deep grooves down in the substrate underneath. We have done some experiments along the lines of the first idea [Schneider97]. We first write a structure in the near field by de-activating molecules of a monomolecular initiator layer covalently bound to the glass substrate. Since this layer is extremely thin, one obtains a very well-defined width about the diameter of the aperture. In the next step we place the sample in a solution of MMA monomers at about 190°. Polymerization under this condition results in polymer brushes which are more densely packed than direct formation of a film out of a polymer solution. Fig. 29 shows some preliminary results. The structure width is still far from what one could expect. The overall process in this experiment is somewhat complicated and there could be many sources for this problem including the polymerization process itself.

V.c Tungsten oxide

The two previous experiments both aimed at a change of surface topography on a nanometer scale. One can also modify the optical constants of a sample without any topography change. Figure 30 shows such an example where we have illuminated a thin layer of tungsten oxide WO_3 [Wegscheider, unpub.]. The film has remained flat

while an optical contrast is produced. The process leading to this effect is a series of chemical reactions initiated by exposure to ultraviolet light [Deb73, Bechinger93]:

$$WO_3 + h\nu \longrightarrow WO_3 + e^- + h^+$$

$$2h^+ + H_2O \longrightarrow 2H^+ + \frac{1}{2}O_2$$

$$2WO_3 + 2e^- + 2H^+ \longrightarrow 2HWO_3$$

The index of refraction as well as the absorption of HWO_3 are different from that of WO_3. By coupling light from a diode laser at 800nm into the same tip that was used for "writing", we can "read" the structures. The experiment of fig. 30 was performed with uncoated fiber tips, and the reading was done in reflection back into an uncoated fiber tip. Although this system delivers a large power, is easy-to-use, and suitable for experiments on opaque samples, the resolution obtained is not diffraction limited (δ~350nm in fig. 30). You might think that this is obvious since there is no aperture to confine the field. But there have been several reports showing microscopy as well as lithography with sub-wavelength resoltuion using uncoated tips [Courjon90, Krausch95, Madsen97]. After a series of systematic studies in Konstanz we now believe that the resolution obtained is diffraction limited and in cases of sub-100nm apparent resolution it is an artifact [Sandoghdar97].

We have tried to extend our experiments on WO_3 to using coated tips, but the small throughput of these probes have limited our success. Our best results were spots of ~170nm after many minutes of illumination.

V.d Overview of SNOL

To summarize the section on optical near-field lithography, one should say that the idea of optically structuring a surface below the diffraction limit and at a relatively low cost is very attractive and perhaps also promising. The biggest potential is possibly in a mix&match process where one uses far field lithography for bigger dimensions of the sample and adds the finer details with a SNOM. There are a few technical problems which prevent us from getting rich overnight !

1) Until today SNOM remains a very slow technique. This lies in the shear-force distance stabilization which relies on the mechanical resonance of the fiber at 20-100kHz.
2) The tips are non-reproducible leading to an unreliable resolution.
3) The transmission is very low leading to long illumination times.
4) The probes are fragile and have very short lifetimes.

V.e Microfabrication as a possible solution for the future of SNOL

Together with some industry and university partners we are currently examining microfabricated SNOM probes as possible breakthrough for near field microscopy as well as lithography. The central idea is the combination of AFM and SNOM. For this one needs a transparent AFM tip which is metal coated with an aperture at the front. Actually, this idea has been around for a few years now, and

some groups have even done some first experiments [van Hulst, Kassing, Noel]. There are several promising aspects of this:

1) The tip fabrication will be done using professional microfabrication techniques. This might result in more reproducible tips.
2) One obtains a larger opening angle in the tip leading to a higher transmission.
3) The scan and tip-sample distance control mechanisms will be that of AFM, more that an order of magnitude faster than conventional SNOM.
4) Microfabrication opens the doors for parallelization.

The last point is particularly interesting since it could reduce the imaging time further by the number of probes involved. From the technical point of view, this is somewhat challenging because one has to control the distance between each individual probe and the sample separately. This problem is already solved by the use of integrated thin piezoelectric actuator and sensor layers on the cantilever. Using this mechanism or similar ones parallel AFM has been already demonstrated. In a parallel SNOM one should also couple light into each probe and detect the emission of each probe separately. In fact, we have to do all this while arranging the neighboring tips with separations well below 100μm. We hope to present a prototype of such a device by the end of this year.

VI Closing Remarks

In conclusion, after more than a decade SNOM is still a very young area. A lot of progress has been made during this time, and one can indeed purchase SNOM devices from several manufacturers. The biggest barrier remains, however, the suitable probe which is capable of high spatial resolution, high throughput, and is reproducible in fabrication. This means most probably moving away from metal-coated optical fiber tips and inventing novel methods for extracting optical information from a sample on a nanometer scale.

References

Ambrose, W. P., Goodwin, P. M., Martin, J. C., and Keller, R. A. (1994a). Alterations of single molecule fluorescence lifetimes in near-field optical microcopy. *Science*, 265:364–367.

Ambrose, W. P., Goodwin, P. M., Martin, J. C., and Keller, R. A. (1994b). Single molecule detection and photochemistry on a surface using near-field optical excitations. *Phys. Rev. Let.* , 72(1):160–163.

Ambrose, W. P. and Moerner, W. E. (1991). Fluorescence spectroscopy and spectral diffusion of single impurity molecules in a crystal. *Nature*, 349:225–227.

Axelrod (1979). *Biophys. J.*, 26:557.

Bethe, H. A. (1944). Theory of diffraction by small holes. *Phys. Rev.*, 66:163–182.

Betzig, E. and Chichester, R. J. (1993). Single molecules observed by near-field scanning optical microscopy. *Science*, 262:1422–1425.

Bouwkamp, C. J. (1950a). On Bethe's theory of diffraction by small holes. *Philips Res. Rep.*, 5:321–332.

Bouwkamp, C. J. (1950b). On the diffraction of electromagnetic waves by small circular disks and holes. *Philips Res. Rep.*, 5(6):401–422.

Casimir, H. B. G. and Polder, D. (1948). *Phys. Rev.*, 73:360.

Davy, S. and Spajer, M. (1996). Near field optics: snapshot of the field emitted by a nanosource using a photosensitive polymer. *Appl. Phys. Lett.*, 69(22):3306–3308.

Decca, R. S., Drew, H. D., and Empson, K. L. (1997). Investigations of the electric field distribution at the subwavelength aperture of a near field scanning optical microscope. *Appl. Phys. Lett.*, 70(15):1932–1934.

Dickson, R. M., Cubitt, A. B., Talen, . Y., and Moerner, W. E. (1997). On/off blinking and switching behaviour of single molecules of green fluorescent protein. *Nature*, 388(3):355–358.

Gammon, D., Snow, E. S., Shanabrook, B. V., Katzer, D. S., and Park, D. (1996). Homogeneous linewidths in the optical spectrum of a single gallium arsenide quantum dot. *Science*, 273:87–90.

Girard, C., Martin, O. J. F., and Dereux, A. (1995). Molecular lifetime changes induced by nanometer scale. *Phys. Rev. Let.* , 75(17):3098–3101.

Granstroem, M., Berggren, M., and Inganaes, O. (1995). *Science*, 267:1479.

Ha, T., Enderle, T., Chemla, D. S., Selvin, P. R., and Weiss, S. (1996a). Single molecule dynamics studied by polarization modulation. *Phys. Rev. Let.* , 77(19):3979–3982.

Ha, T., Enderle, T., Ogletree, D. F., Chemla, D. S., Selvin, P. R., and Weiss, S. (1996b). Probing the interaction between two single molecules: Fluorescence resonance energy transfer between a single donor and a single acceptor. *Proc. Natl. Acad. Sci. USA*, 93:6264–6268.

Hinds, E. A. (1991). *Adv. Atom. Mol.Opt.Phys.*, 28:237.

Hinds, E. A. and Sandoghdar, V. (1991). Cavity QED level shifts of simple atoms. *Phys. Rev. A*, 43(1):398–403.

Jackson, J. D. (1975). *Classical Electrodynamics*. Wiley, New York.

Jung, T. A., Schlittler, R. R., Gimzewski, J. K., Tang, H., and Joachim, C. (1996). *Science*, 271:181.

Kador, L. (1995). Recent results of single-molecule spectroscopy in solids. *Phys. Stat. Sol. (B)*, 189(1):11–36.

Kopelman, R. and Tan, W. (1993). Near-field optics: Imaging single molecules. *Science*, 262:1382.

Krausch, G., Wegscheider, S., Kirsch, A., Bielefeldt, H., Meiners, J., and Mlynek, J. (1995). Near-field microscopy and lithography with uncoated fiber tips: a comparison. *Opt. Comm.*, 119:283.

Kuck, N., Lieberman, K., and Lewis, A. (1992). *Appl. Phys. Lett.*, 61:139.

Lennard-Jones, J. E. (1932). *Trans. Faraday Soc.*, 28:333.

Lewis, A. (1995). Near field optics. Winter College on Optics, Trieste.

Lewis, A. and Lieberman, K. (1991). *Nature*, 254:214.

London, F. (1930). *Z. Physik*, 63:245.

Loudon, R. (1986). *The Quantum Theory of Light*. Oxford University Press.

Lu, H. P. and Xie, X. S. (1997). Single molecule spectral fluctuations at room temperature. *Nature*, 385:143–146.

Lukosz, W. and Kunz, R. E. (1977). Fluorecence of magnetic and electric dipoles near a dielectric interface. *Opt. Commun.*, 20(2):195–199.

Macklin, J. J., Trautman, J. K., Harris, T. D., and Brus, L. E. (1996). Imaging and time-resolved spectroscopy of single molecules at an interface. *Science*, 272:255–258.

Madsen, S., Bozhevolnyi, S., Birkelund, K., Mllenborn, M., Hvam, J. M., and Grey, F. (1997). Oxidation of hydrogen-passivated silicon surfaces by scanning near-field optical lithography using uncoated and aluminum-coated fiber probes. *J. Appl. Phys.*, 82:49.

Margenau, H. (1939). *Rev. Mod. Phys.*, 11:1.

Moerner, W. E. (1994). Examining nanoenvironments in solids on the scale of a single, isolated impurity molecule. *Science*, 265:46–53.

Moerner, W. E. (1996). *Acc. Chem. Res.*, 29:563.

Moerner, W. E. and Kador, L. (1989). Optical detection and spectroscopy of single molecules in a solid. *Phys. Rev. Let.* , 62(21):2535–2538.

Monroe, C. (1996). *Acc. Chem. Res.*, 29:585.

Morawitz, H. (1969). *Phys. Rev.*, 187:1792.

Novotny, L. (1996). Single mlecule fluorescence in inhomogeneous environments. *Appl. Phys. Lett.*, 69(25):3806–3808.

Nyffenegger, R. M. and Penner, R. M. (1997). *Chemical Reviews*, 97(4):1195.

Orrit, M. and Bernard, J. (1990). Single pentacene molecules detected by fluorescence excitation in a p-therphenyl crystal. *Phys. Rev. Let.* , 65:2716.

Purcell, E. M. (1946). *Phys.Rev.*, 69:681.

Rahmani, A., Chaumet, P. C., de Fornel, F., and Girard, C. (1997). Field propagator of a dressed junction: fluorescence lifetime calculations in confined geometry. *Phys. Rev. A*, ???(?):??

Ruiter, A. G., Veerman, J. A., Garcia-Parajo, M. F., and van Hulst, N. F. (1997). Single molecule rotational and translational diffusion observed by near-field scanning optical microscopy. *J. Phys. Chem.*, 101:7318.

Sandoghdar, V., Sukenik, C., Haroche, S., and Hinds, E. (1996). Spectroscopy of atoms confined to the single node of a standing wave in a parallel-plate cavity. *Phys. Rev. A*, 53:1919.

Sandoghdar, V., Sukenik, C., Hinds, E., and Haroche, S. (1993). Direct measurement of the van der waals interaction between an atom and its images in a micron-sized cavity. *Phys. Rev. Lett.*, 68(23):3432.

Sandoghdar, V., Wegscheider, S., Krausch, G., and Mlynek, J. (1997). Reflection scanning near-field optical microscopy with uncoated fiber tips: How good is the resolution really? *J. Appl. Phys.* 81 : 2499.

Schneider, B. (1997). Nanolithography on polymer brushes. Master's thesis, University of Konstanz.

Sekatskii, S. K. and Letokhov, V. S. (1996). Single fluorescence centers on the tips of crystal needles: first observation and prospects for application in scanning one-atom fluorescence microscopy. *Appl. Phys. B*, 63:525–530.

Stroscio, J. and Eigler, D. M. (1991). *Science*, 254:1319.

Sukenik, C. I., Boshier, M. G., Cho, D., Sandoghdar, V., and Hinds, E. A. (1993). *Phys. Rev. Lett.*, 70:560.

Trautman, J. K. and Macklin, J. J. (1996). Time-resolved spectroscopy of single molecules using near-field and far-field optics. *J. Chem. Phys*, 205:221–229.

Trautman, J. K., Macklin, J. J., Brus, L. E., and Betzig, E. (1994). Near-field spectroscopy of single molecules at room temperature. *Nature*, 369:40–42.

Vorwerk, M. (1996). Single molecule detection in the optical near field. Master's thesis, University of Konstanz.

Waggon, U. (1997). *Optical properties of semiconductor quantum dots*, volume 136 of *Springer Tracts in Modern physics*. Springer, Heidelberg, Germany.

Wegscheider, S., Kirsch, A., Mlynek, J., and Krausch, G. (1995). Scanning near-field optical lithography. *Thin Solid Films*, 264:264–267.

Xie, X. S. and Dunn, R. C. (1994). Probing single molecule dynamics. *Science*, 265:361–364.

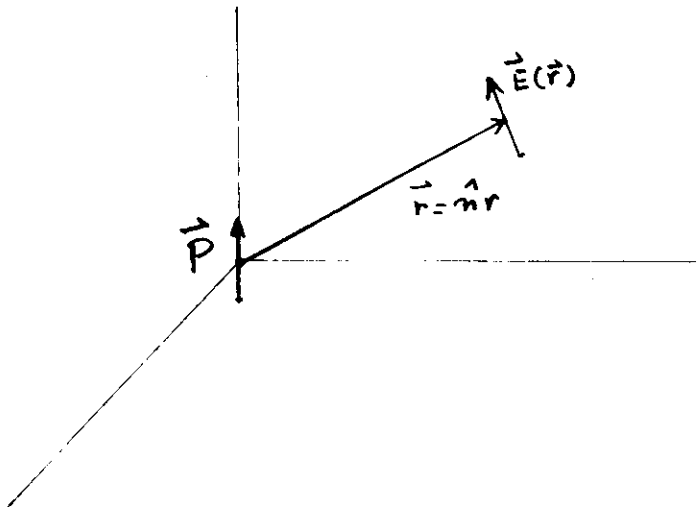

Fig. 1

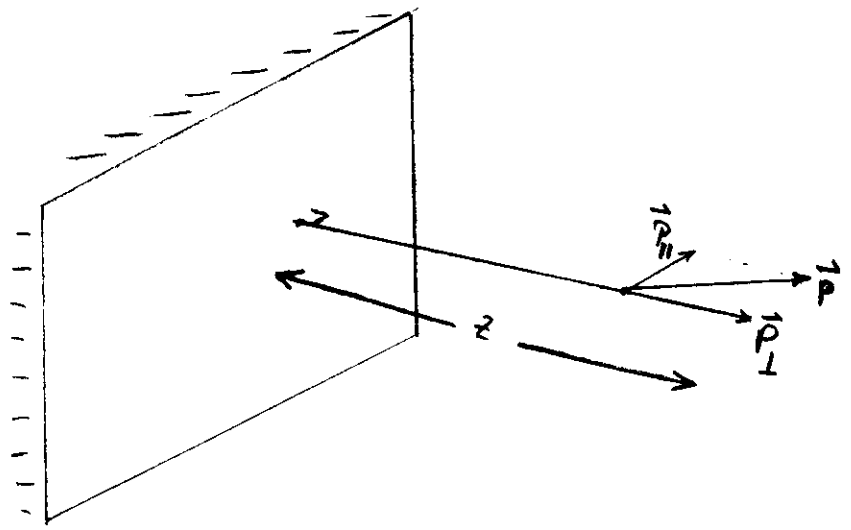

Fig. 2

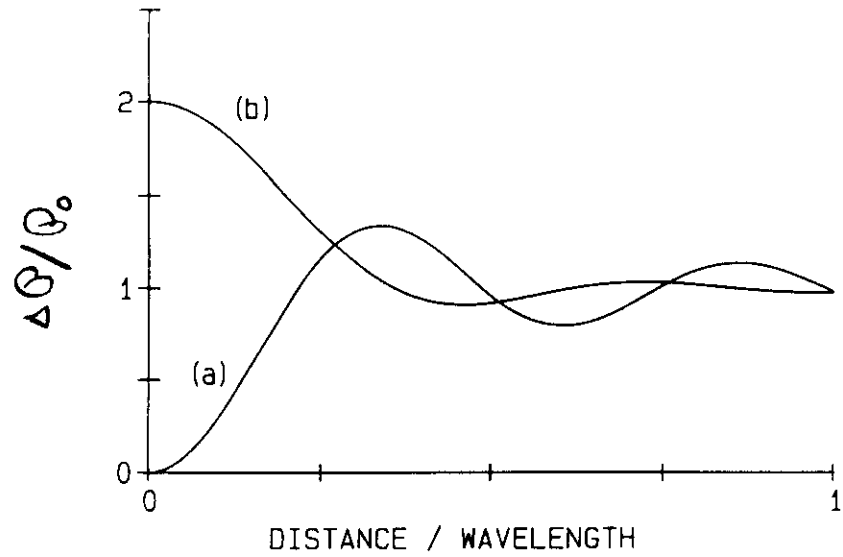

Fig. 3 The change in radiated power normalized to the free space power $\mathcal{P}_0$ of a classical dipole moment as a function of its distance to the mirror normalized to the wavelength of oscillation. (a) is a dipole parallel to and (b) is perpendicular to the mirror.

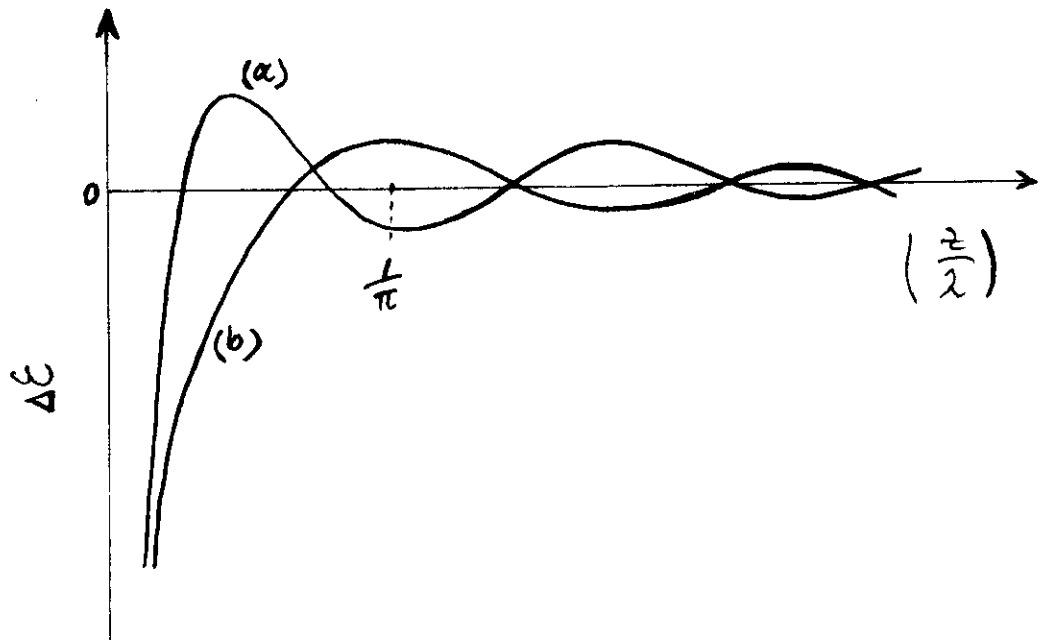

Fig. 4 The shift of dipole's energy (in arbitrary units) for parallel (a) and perpendicular (b) dipoles as a function of normalized distance to the mirror. Close to the interface both diverge.

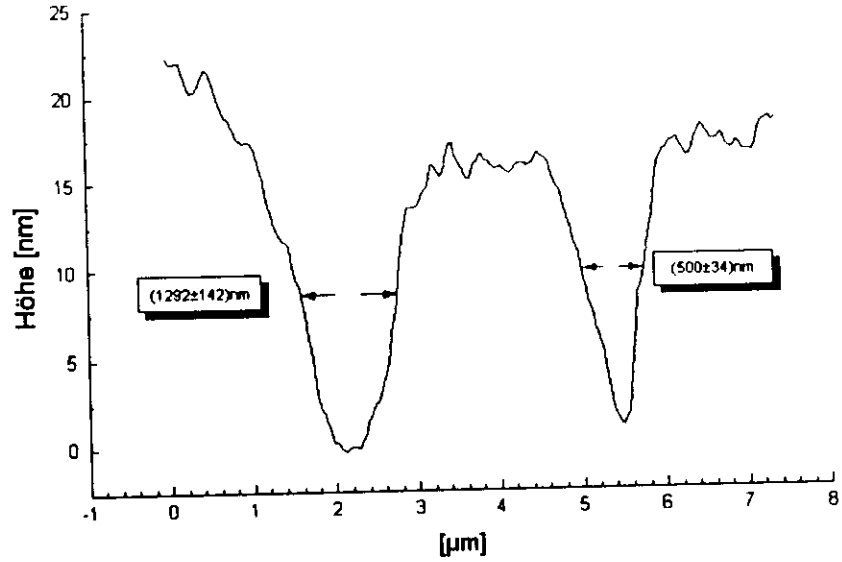

Fig.29 Cross-section of the topography profile obtained by the radical polymerization process discussed in the text. The structure at the right is the result of a single pass illumination while the one at the left was obtained when two lines with separations of about 500nm were scanned and illuminated.

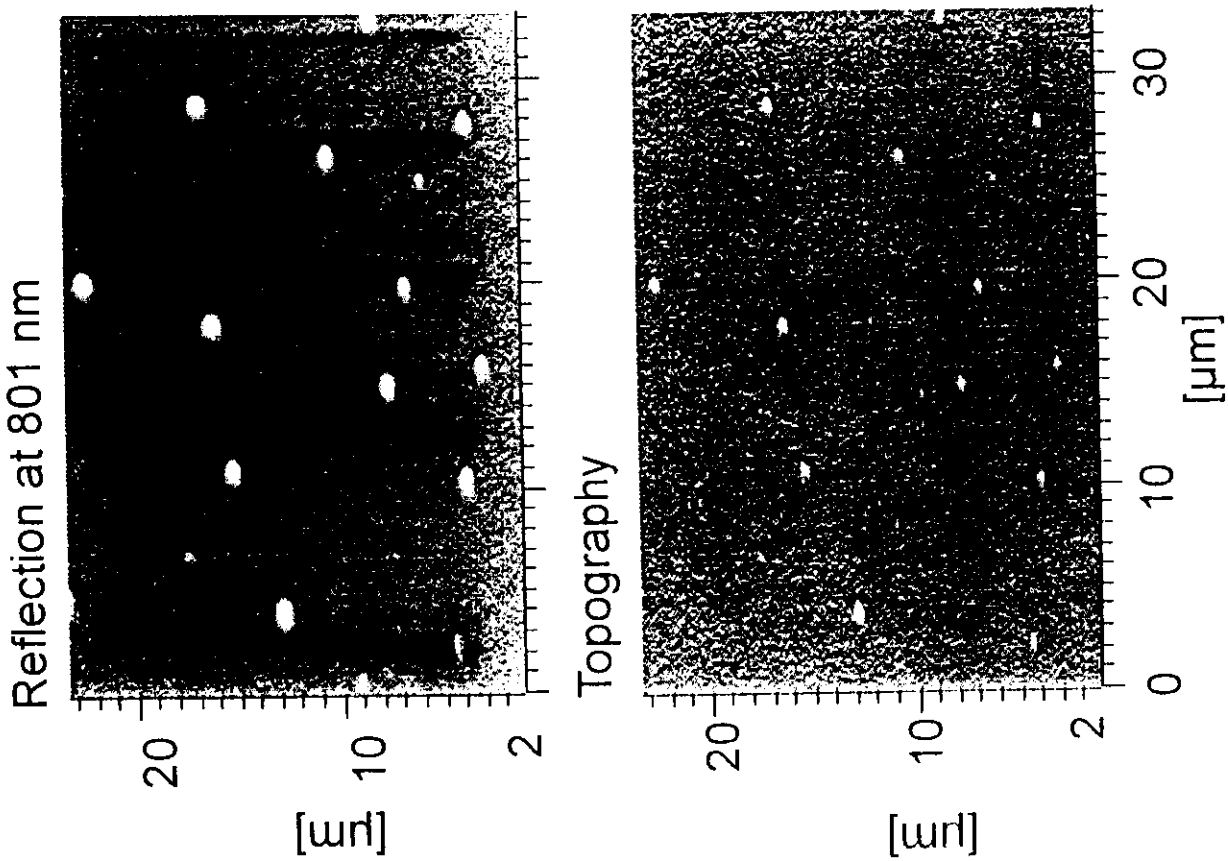

Fig.30 Top: The intensity of the light (λ=801nm) reflected back into the uncoated fiber. The darker areas indicate higher local absorption of HWO_3. Bottom: The topography of the sample recorded at the same time; it remains flat. The white spots are dust particles !

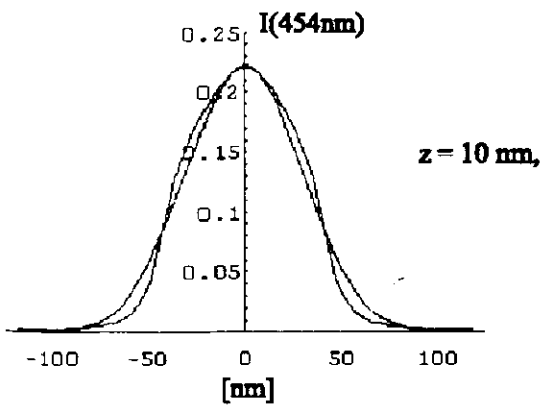

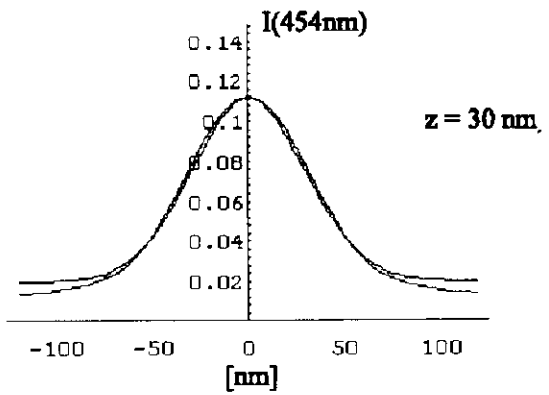

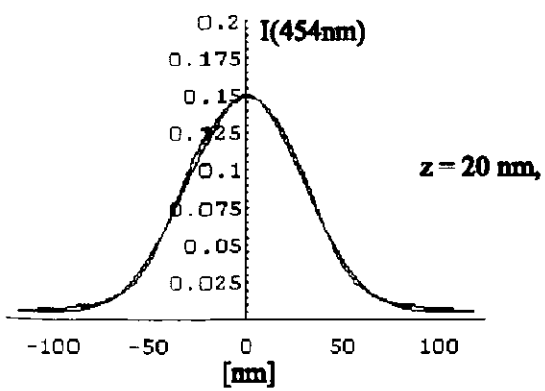

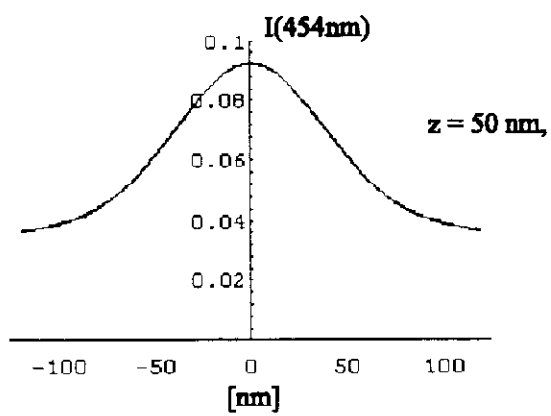

Fig.28 Intensity profiles at different distances z from the tip for an aperture of a=100nm. Note that at z=20 the profile is very well approximated by a Gaussian of FWHM=80nm.

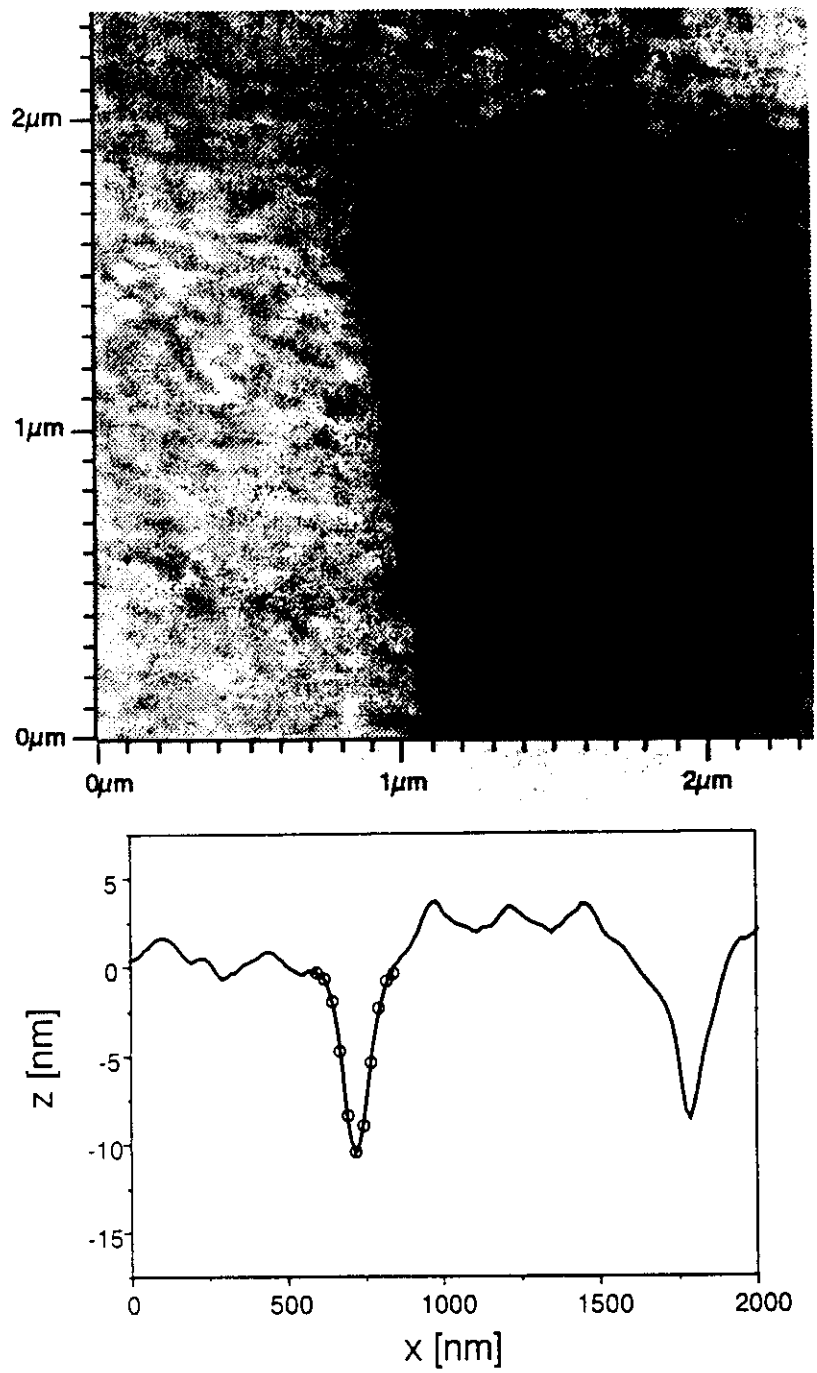

AFM images of line pattern created by SNOL in a standard photo resist. (a) Top view of a set of parallel lines created by 'single path exposure' through the tapered tip of an optical fiber (for details, see text). (b) Cross-sectional view of single lines; the open circles represent a least-squares fit of a Gaussian profile to the data.

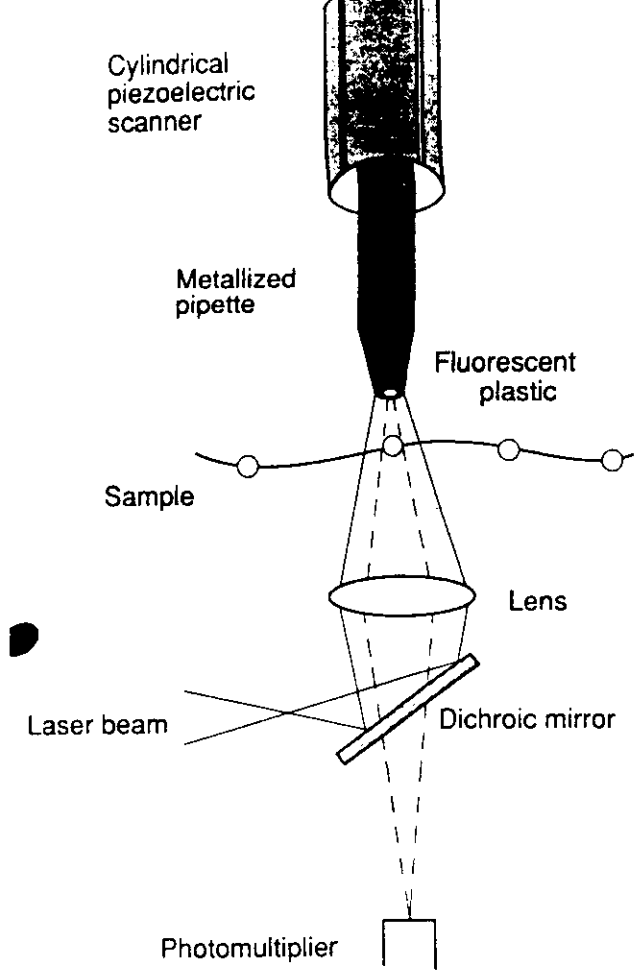

Fig.25 The setup used by A. Lewis in experiments using a metal-coated fiber stuffed with some fluorescing polymer. Note that the excitation was done in the far field and not through the fiber.

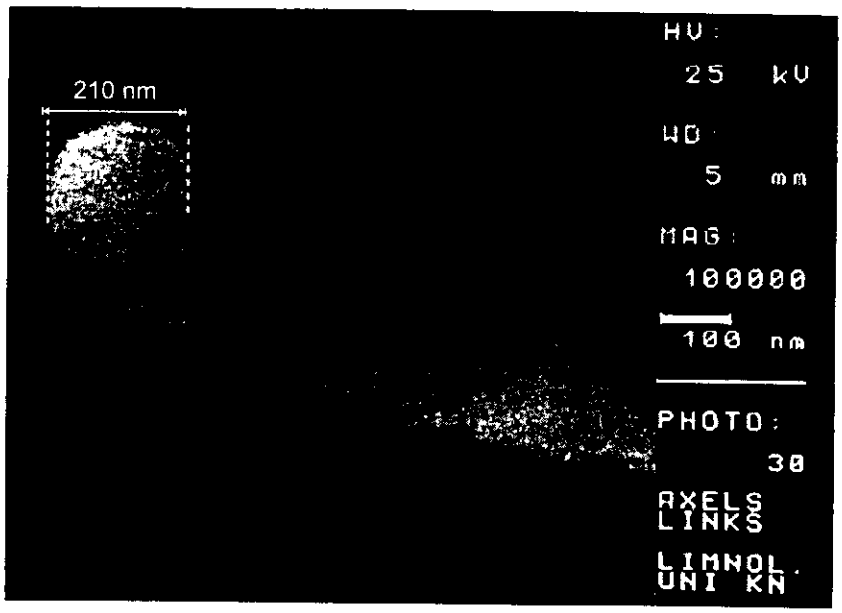

Fig.26 An electron microscope image of a glass fiber tip with a small amount of Eu-doped PMMA at the end.

Fig.21 The molecule in the lower left shows a good example of blinking in single molecule detection. The molecule is turned off suddenly and then turned back on at a later time.

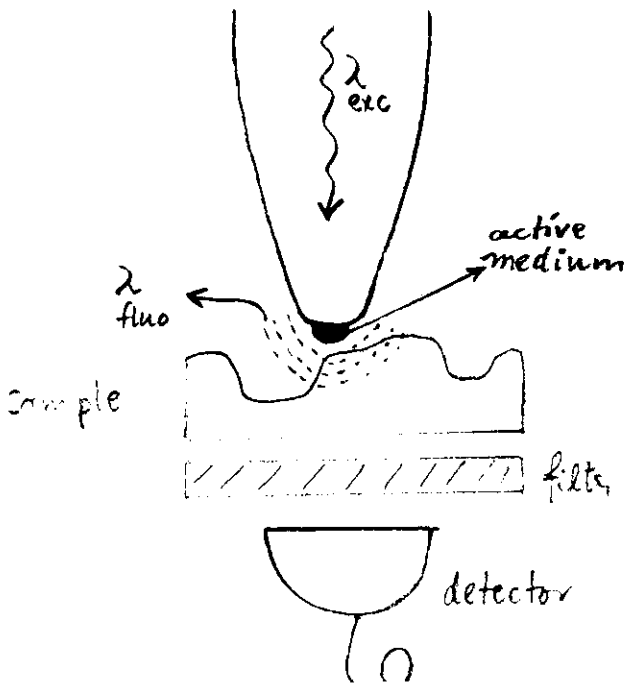

Fig.22 A schematic view of a nanoscopic fluorescence center at the extremity of a sharp tip. By placing the sample very close to this medium one can scatter the non-propagating components of the fluorescence.

Fig.24 Schematics of the arrangement for choosing a single molecule in a small matrix as an emitter for optical near-field microscopy

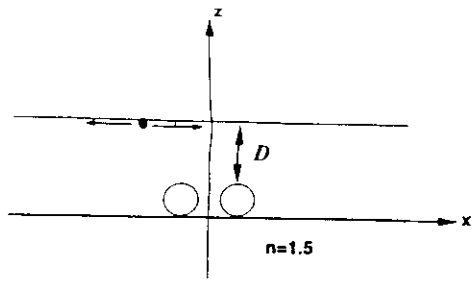

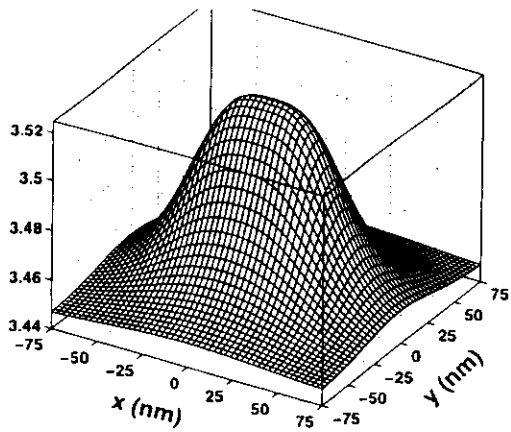

D=40 nm

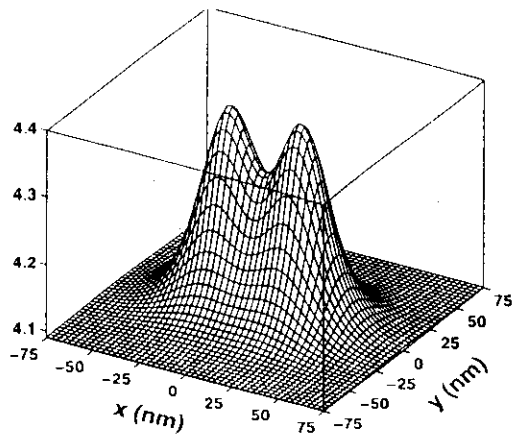

D = 20 nm

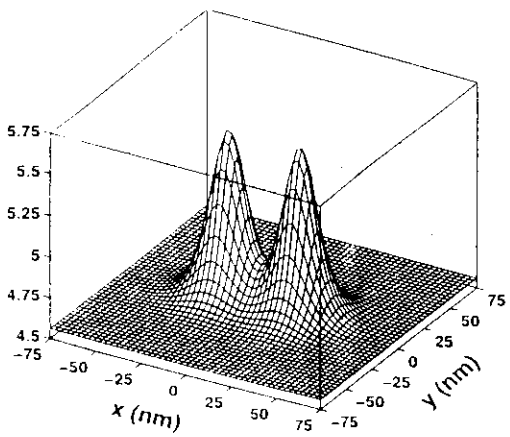

D = 10 nm

Fig.23 Simulations showing the modification of lifetime of a single molecule when placed scanned across two glass spheres. The results for three different separations are shown (taken from [Rahmani et al.]).

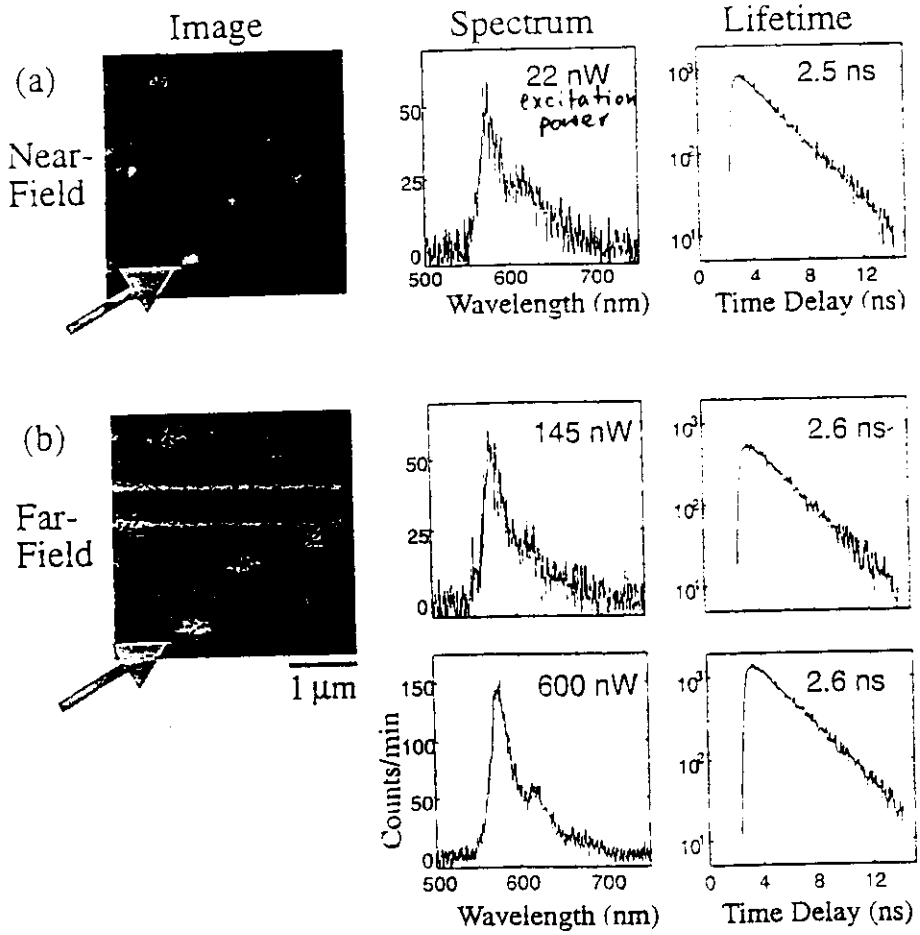

Fig.19 The comparison of the spectra and the lifetime measured from the *same* molecules in the near field as well as far field. In this case there is no obvious perturbation caused by the tip (taken from [Trautman&Macklin]).

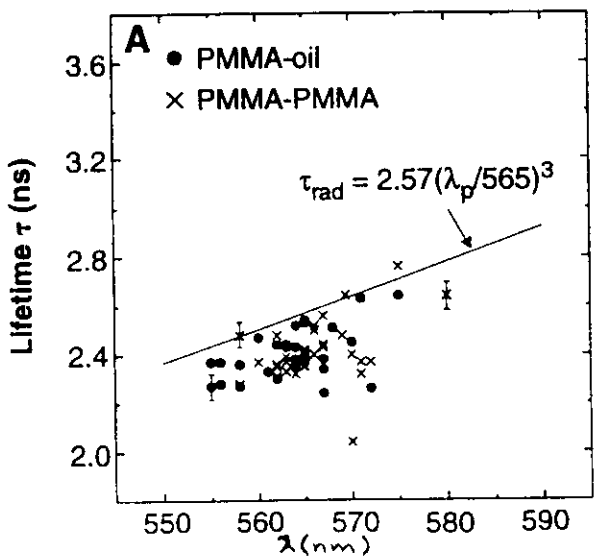

Fig.20 The lifetimes measured for many different molecules plotted against the peak wavelength in their spectra. The solid line depicts the dependence one would expect from the third power wavelength dependence of the spontaneous emission rate (taken from [Macklin et al.96]).

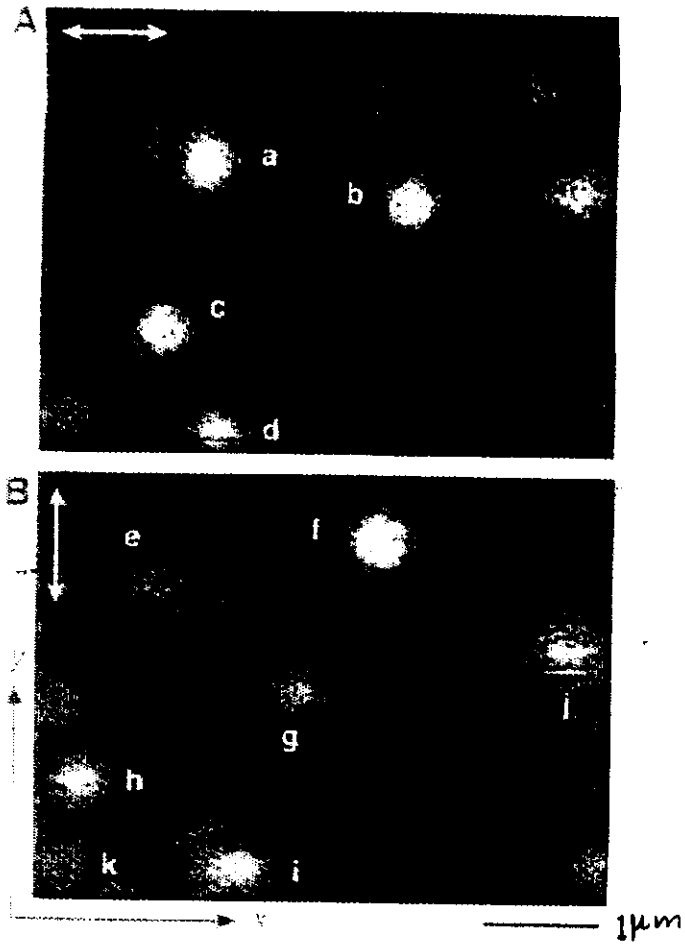

Fig.17 Some images taken in the confocal mode using the setup shown in fig. 16. The polarization of the excitation is shown by the white arrows in each case.

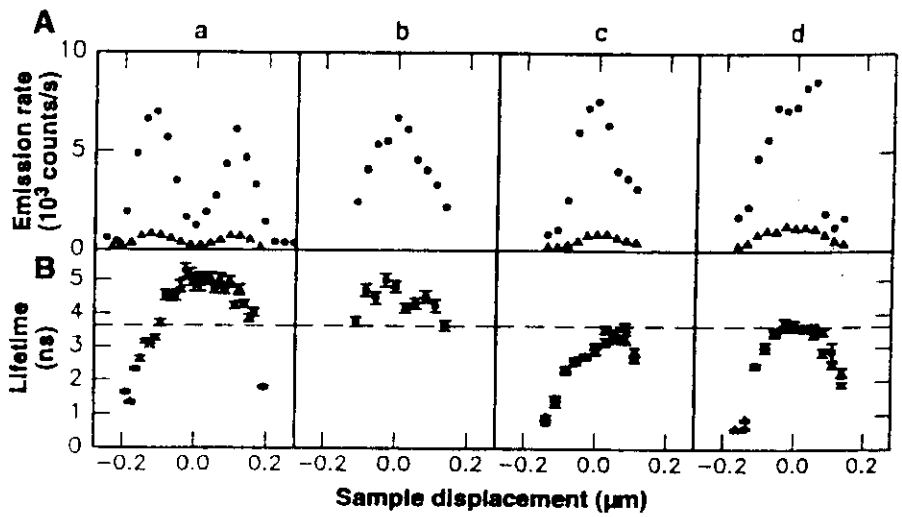

Fig. 18 (**A**) Emission rate and (**B**) fluorescence lifetime versus lateral displacement for four different R6G molecules (a through d). Molecule a corresponds to feature a in Fig. 1. We relocated single molecules identified in image scans using a search routine while monitoring the fluorescence signal. The tip was maintained <10 nm from the surface throughout these measurements (the height noise was ~2 nm peak to peak). At each position separated by ~27 nm, 7938 photocounts were obtained. Error bars on the τ data are confidence limits on single exponential fits. Far-field power levels: molecule a, (●) 22 and (▲) 2.5 nW; molecule b, (●) 38 nW; molecule c, (●) 31 and (▲) 3.8 nW; and molecule d, (●) 42 and (▲) 4.9 nW.

taken from Ambrose et al. in Science

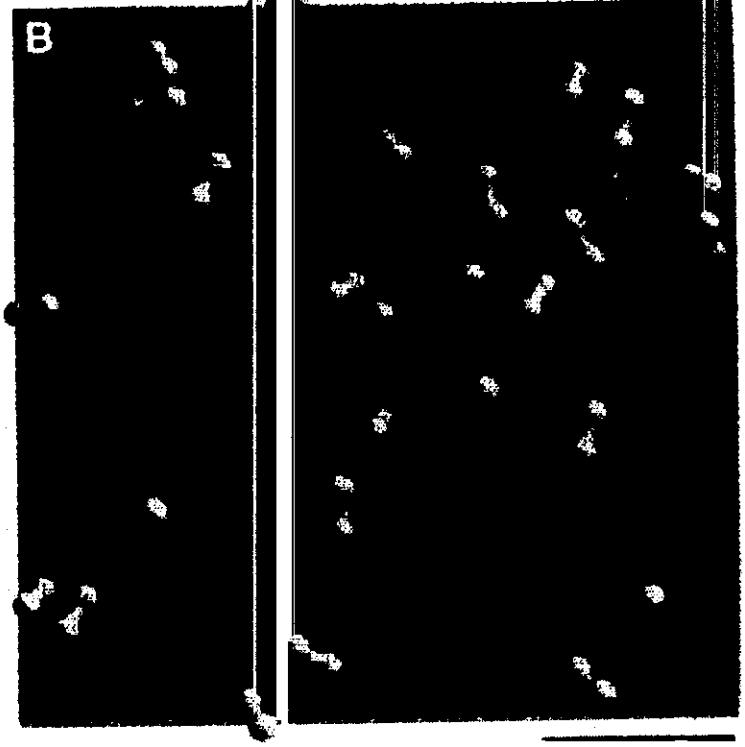

Fig.15 The same image as that shown in fig. 11, but after the analysis of absorption dipole orientation. A molecular dipole moment is represented by a dumbbell.

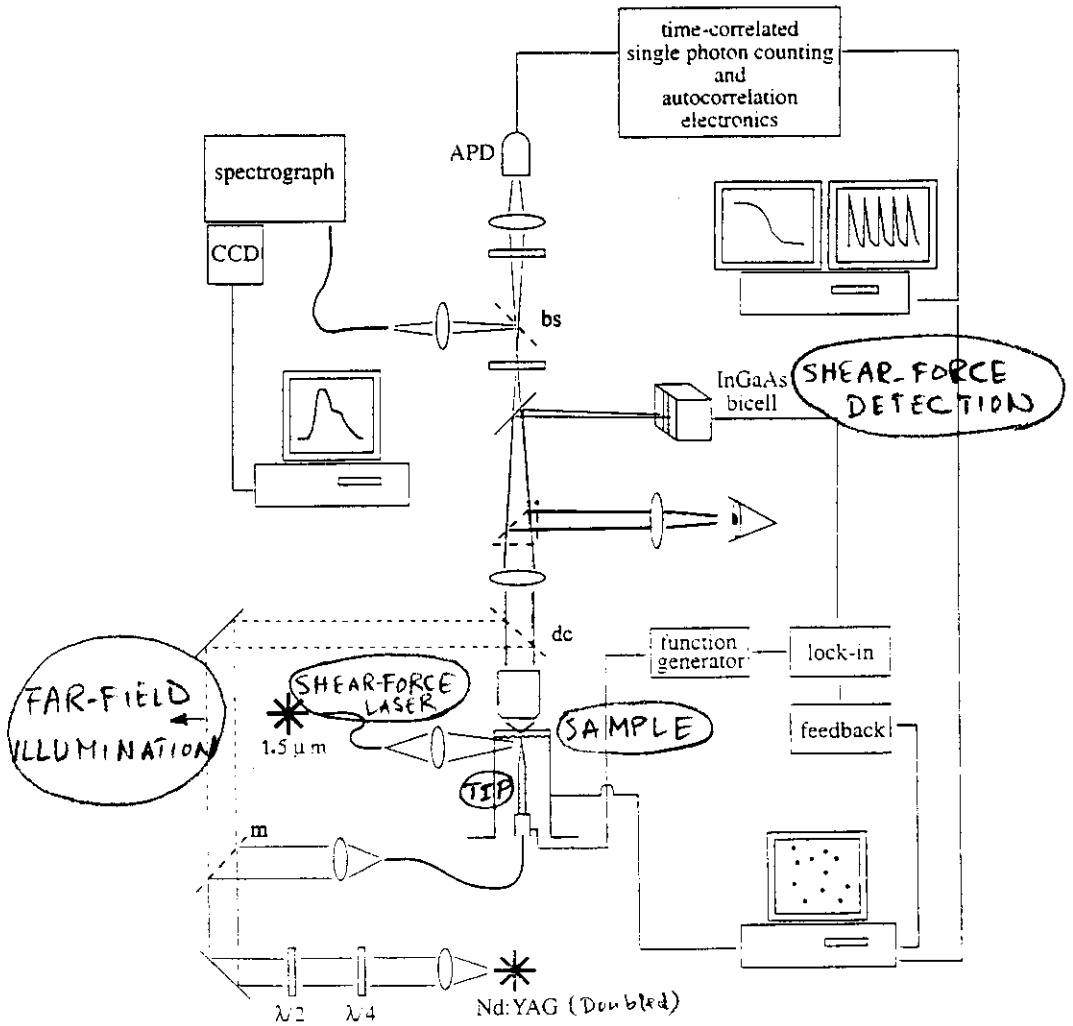

Fig.16 The schematics of the combined far-field/near-field microscope used by Trautman to study the effects that might be induced by the tip.

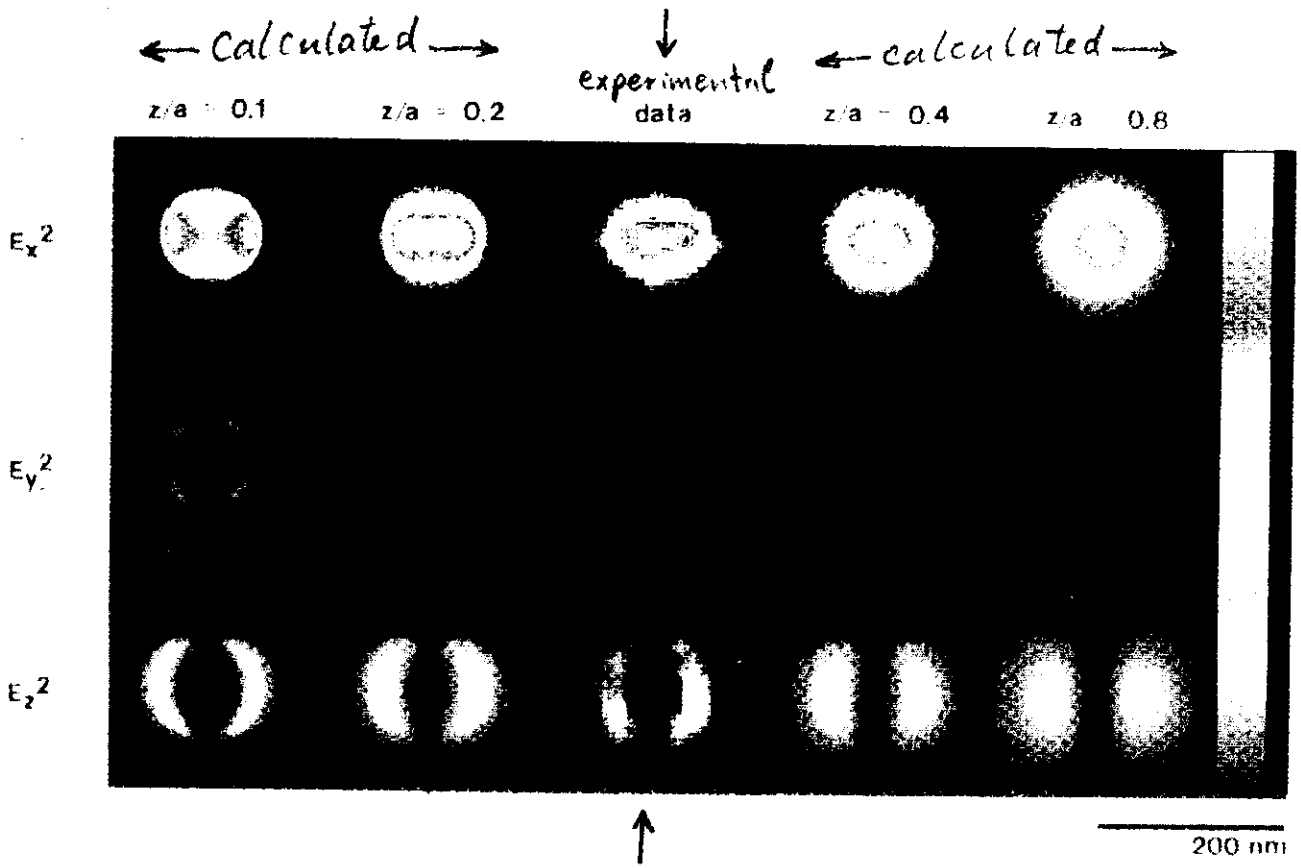

Fig.14 The calculated intensity profiles in three directions similar to those in fig. 12 for four various distances from the tip. In the middle Betzig and Chichester have placed their experimentally observed data for two molecules which happened to be oriented along x or z directions (taken from [Betzig&Chichester93]).

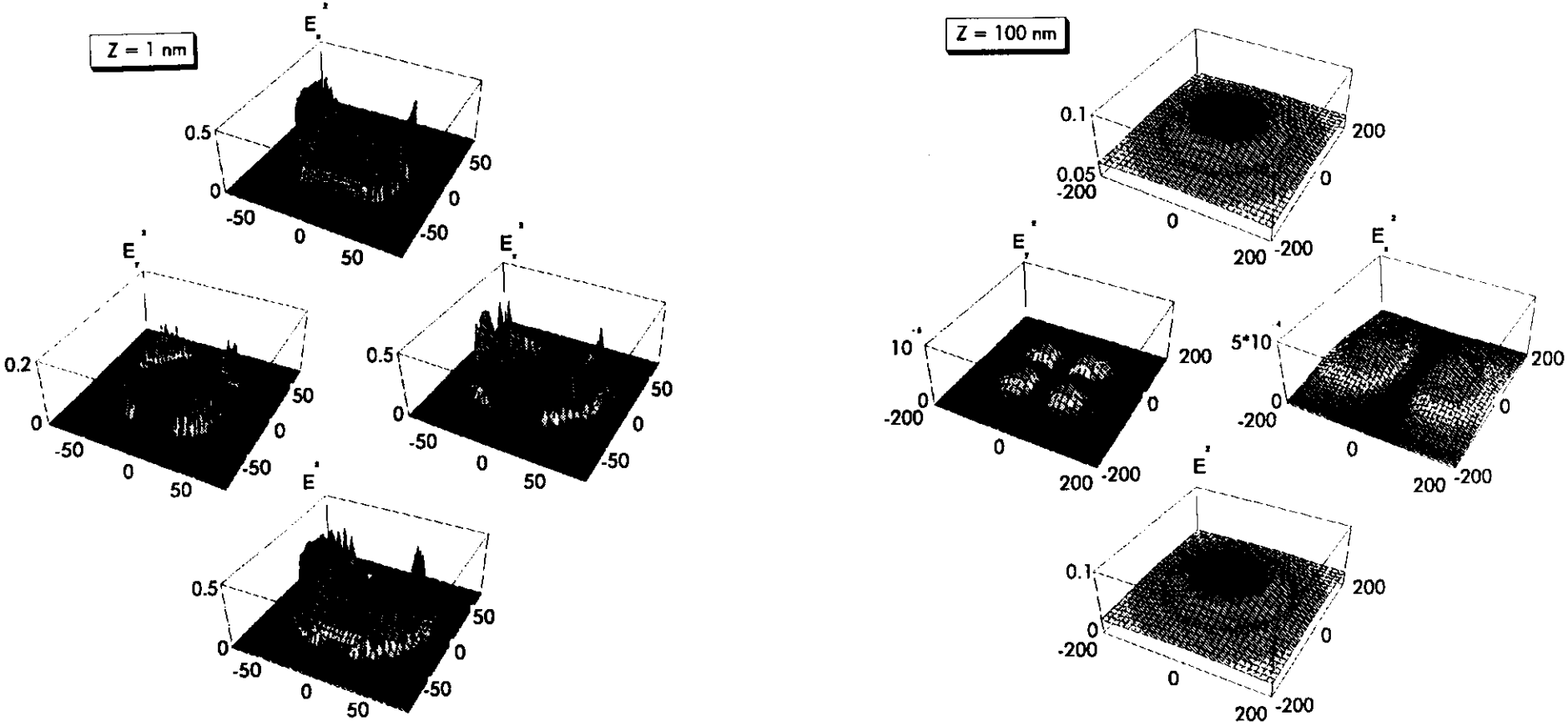

Fig.13 The square of the electric field in all three directions as well as their sum is calculated using the B&B theory. The aperture a was taken to be 100nm and the light in the fiber tip was taken to be polarized along the x-axis. Z is the distance from the aperture at which the field is plotted.

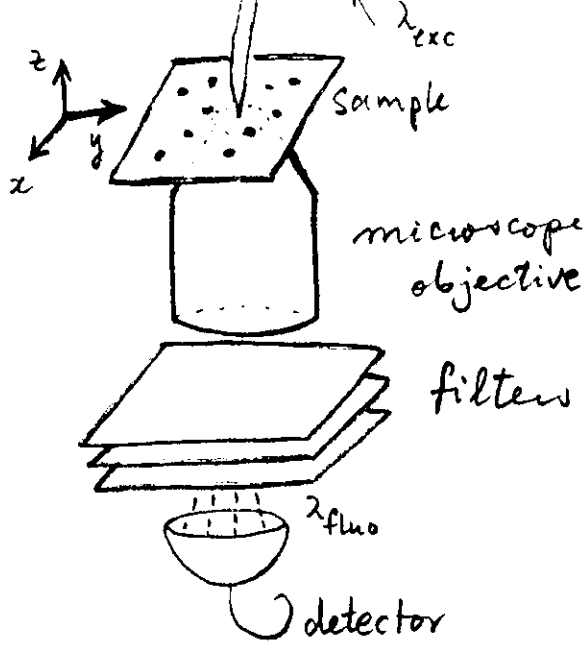

Fig.10 The schematics of the setup for the detection of single molecules on a surface using a SNOM. The excitation light is coupled into a metal-coated optical fiber tip. The sample is scanned in three directions while the fluorescence is collected by a high numerical aperture microscope objective. By using high quality filters one can eliminate unwanted light such as that of the excitation.

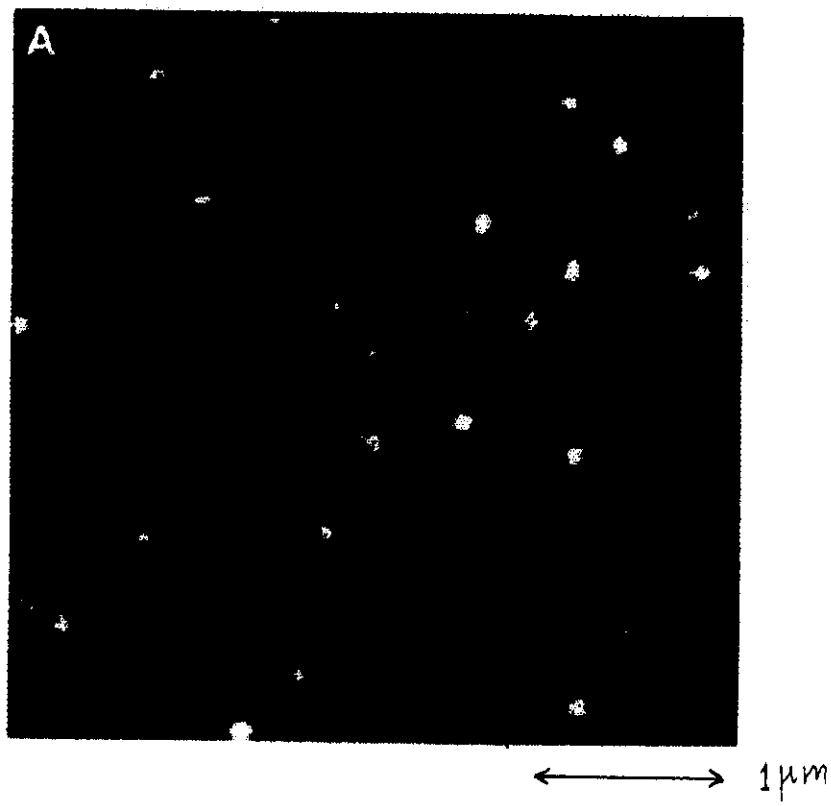

Fig.11 An example of the images one obtains from the experiment discussed in figure 10. The bright spots correspond to single dye molecules.

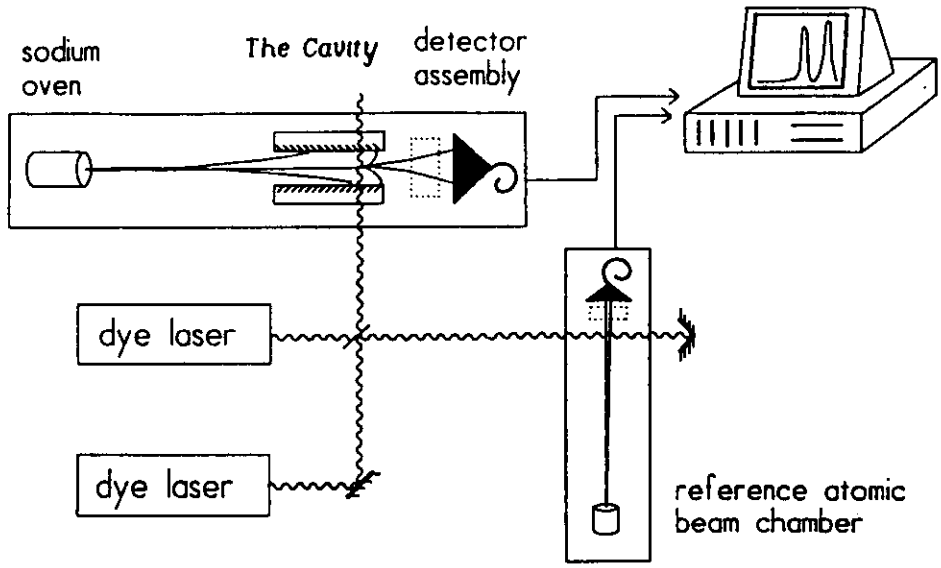

Fig. 8 The schematics of the experimental setup. Two atomic beam machines are shown together with two dye lasers. The atoms in the reference beam are unperturbed and can be excited from 3S to nS state (n=10-13) in a resonant two-step process. Atoms in the main beam have to travel through the cavity formed by the two mirrors and are excited shortly before the exit. Due to the interaction with the mirrors the energy levels are shifted. The shift is measured by comparing the spectra taken simultaneously from the two atomic beam machines.

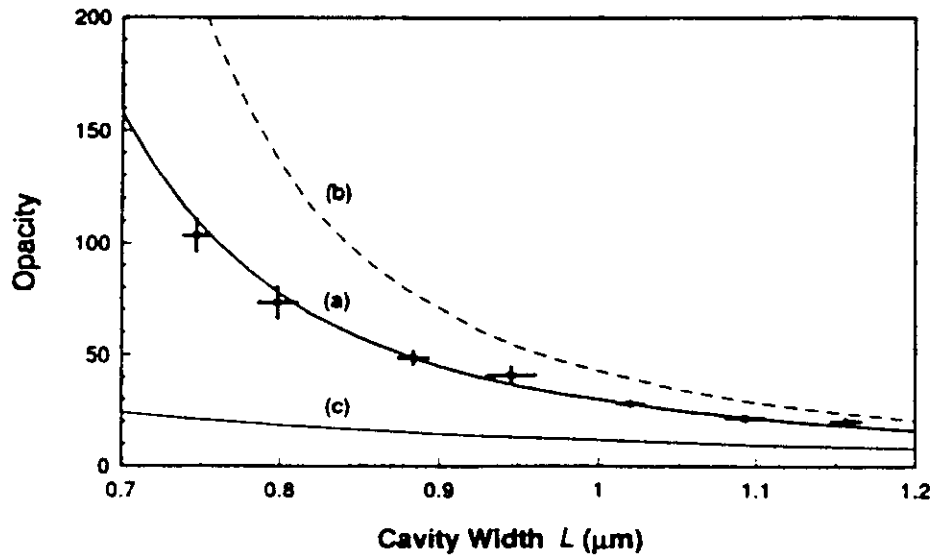

Fig. 9 Some of the results of the experiment performed by Sukenik et al. to put into evidence the long range retarded Casimir-Polder forces. The set up was essentially the same as that in fig. 8, but the atoms were excited outside the cavity. In this way the transmitted ground state atoms were simply counted for various cavity widths. The plate separation was of the order of one micron and therefore much larger than λ/π for the transition between 3S and 3P of sodium. This means that the interaction between the atoms and the mirrors is in the far field regime. The crosses in the figure show the experimental results of the inverse of the number of atoms which survived the cavity force. Solid line (a) is the expected curve based on a full quantum mechanical treatment of Casimir and Polder. Curve (b) is what one expects from an instantaneous Lennard-Jones van der Waals, and curve (c) the purely geometrical effect of the cavity solid angle on the transmission of the atoms. The clear deviation of the interaction from a simple electrostatic one (the difference between (a) and (b)) is shown for the first time.

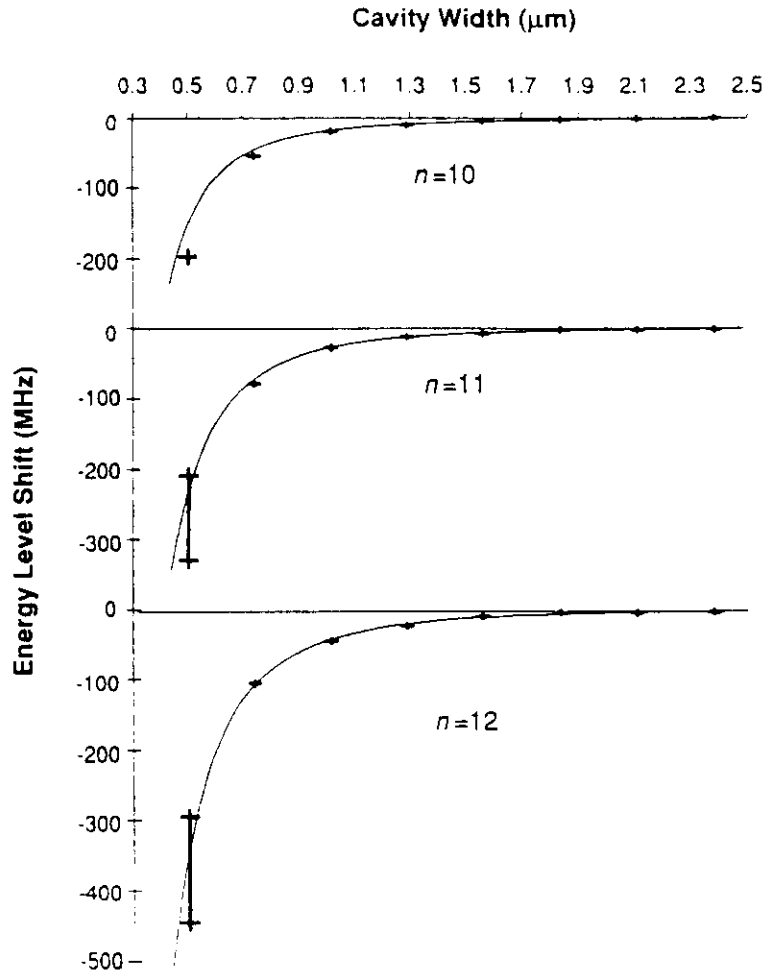

Fig. 7 Experimentally measured energy level shifts of sodium atoms between two parallel mirrors. The x-axis shows the separation between the two plates. The experiment was performed on atoms in three different atomic states n=10,11,12 and for eight mirror separations. The relevant transition wavelengths for atoms in these states are few tens of microns; this means that plate separations of about one micron puts us in the near field regime. The solid lines plot the theoretically expected shifts (see equations 10 and 11) without any free parameters. For the experimental setup see fig. 8.

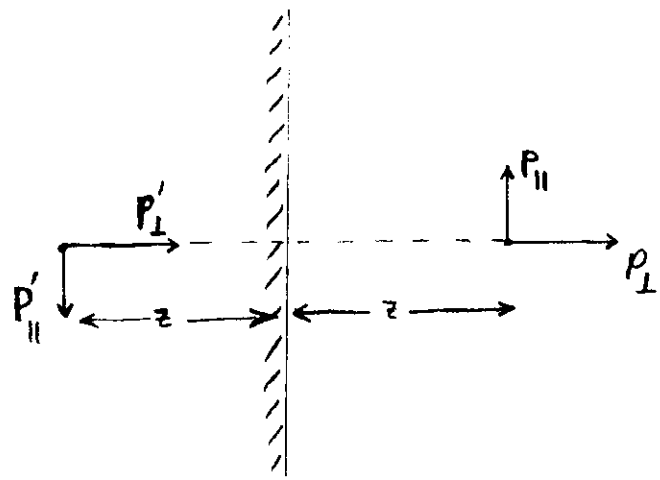

Fig. 5 The dipole **p** is shown with its mirror image dipole **p'**. Note the difference in sign when **p** is parallel or perpendicular to the mirror.

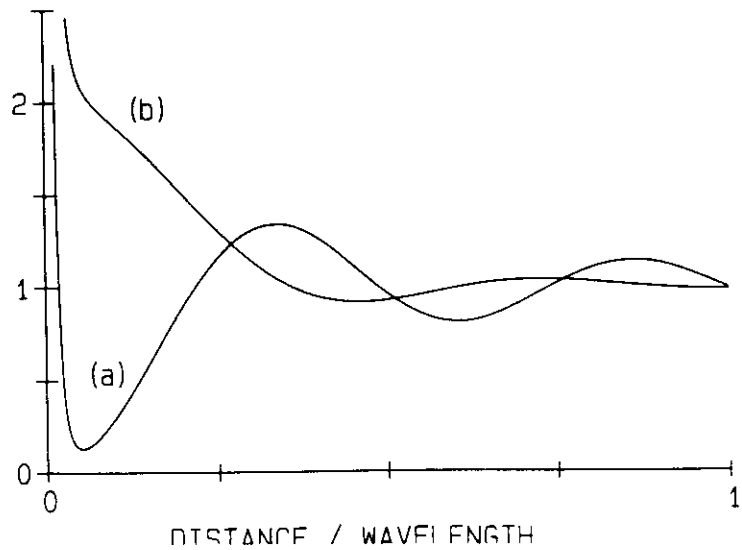

Fig.6 The same as in fig. 3 but with a slightly lossy metallic mirror instead of a perfect mirror. Close to the surface the radiated power diverges for both dipole orientations due to the coupling of the near field with electrons in the metal.